PHYSICAL REVIEW D **86,** 114039 (2012)

Diffractive gauge bosons production beyond QCD factorization

R. S. Pasechnik*
Department of Astronomy and Theoretical Physics, Lund University, SE 223-62 Lund, Sweden

B. Z. Kopeliovich and I. K. Potashnikova
Departamento de Física Universidad Técnica Federico Santa María, Instituto de Estudios Avanzados en Ciencias e Ingeniería, and Centro Científico-Tecnológico de Valparaíso, Casilla 110-V, Valparaíso, Chile
(Received 29 April 2012; published 28 December 2012)

We discuss single diffractive gauge boson ($\gamma^*, W^{\pm}, Z$) production in proton-proton collisions at different (Large Hadron Collider and Relativistic Heavy Ion Collider) energies within the color dipole approach. The calculations are performed for gauge bosons produced at forward rapidities. The diffractive cross section is predicted as a function of the fractional momentum and invariant mass of the lepton pair. We found a dramatic breakdown of the diffractive QCD factorization caused by an interplay of hard and soft interactions. Data from the CDF experiment on diffractive production of W and Z are well explained in a parameter-free way.

DOI: 10.1103/PhysRevD.86.114039 PACS numbers: 13.87.Ce, 14.65.Dw

I. INTRODUCTION

The characteristic feature of diffractive processes at high energies is the presence of a large rapidity gap between the remnants of the beam and target. The general theoretical framework for such processes was formulated in the pioneering works of Glauber [1], Feinberg and Pomeranchuk [2], and Good and Walker [3]. The new *diffractive* state is produced only if different Fock components of the incoming plane wave, which are the eigenstates of interaction, interact differently with the target. This results in a new combination of the Fock components, which can be projected to a new physical state (e.g., see the review on QCD diffraction in Ref. [4]).

The main difficulty in the formulation of a theoretical QCD-based framework for diffractive scattering arises from the fact that it is essentially contaminated by soft, nonperturbative interactions. For example, diffractive deep-inelastic scattering (DIS), $\gamma^* p \to Xp$, although it is a higher twist process, is dominated by soft interactions [5]. Within the dipole approach [6], such a process looks like elastic scattering of $\bar{q}q$ dipoles of different sizes and of higher Fock states containing more partons. Although formally the process $\gamma^* \to X$ is an off-diagonal diffraction, it does not vanish in the limit of unitarity saturation, the so-called black-disk limit. This happens because the photon distribution functions and hadronic wave functions are not orthogonal. Such a principal difference between diffractive processes in DIS and hadronic collisions is one of the reasons for breakdown of diffractive QCD factorization based, e.g., on the Ingelman-Schlein model [7]. In particular, the cross section of diffractive production of the W boson was found in the CDF experiment [8,9] to be 6 times smaller than was predicted by relying on factorization and HERA data [10]. The phenomenological models based on assumptions of the diffractive factorization, which are widely discussed in the literature (see, e.g., Refs. [11,12]), predict a significant increase of the ratio of the diffractive to inclusive gauge boson production cross sections with energy. This is supposed to be tested soon at the LHC.

The process under discussion, diffractive Abelian radiation of electroweak gauge bosons, is the real off-diagonal diffraction. It vanishes in the black-disk limit and may be strongly suppressed by the absorptive corrections even being far from the unitarity bound. The suppression caused by the absorptive corrections, also known as the survival probability of a large rapidity gap, is related to the initial and final state interactions. Usually, the survival probability is introduced in the diffractive cross section in a probabilistic way and is estimated in oversimplified models, like eikonal, quasieikonal, two-channel approximations, etc. The advantage of the dipole approach is the possibility to calculate directly (although in a model-dependent way) the full diffractive amplitude, which contains all the absorption corrections, because it employs the phenomenological dipole cross section fitted to data. Below, we explicitly single out from the diffractive amplitude the survival probability amplitude as a factor.

Another source of factorization breaking is the simple observation that diffractive Abelian radiation by a quark vanishes in the forward direction (zero momentum transfer to the target) [13]. Indeed, the Fock components of the quark with or without the Abelian boson (γ^*, Z, W, or Higgs boson) interact with the same total cross sections, because only the quark interacts strongly. Therefore, after integration of the amplitude over the impact parameter, the Fock state decomposition of the projectile remains unchanged, and only elastic qp scattering is possible. Notice that non-Abelian radiation (gluons) does not expose this property, because the Fock components $|q\rangle$ and $|qg\rangle$,

*Roman.Pasechnik@thep.lu.se

although they have the same color, interact differently [13,14].

In the case of pp collisions, the directions of propagation of the proton and its quarks do not coincide. Already this is sufficient to get a nonvanishing diffractive Abelian radiation in forward scattering. Moreover, interaction with the spectator partons opens new possibilities for diffractive scattering; namely, the color exchange in the interaction of one projectile parton can be compensated (neutralized) by interaction of another projectile parton. It was found in Refs. [15,16] that this contribution leads to a dominant contribution to the diffractive Abelian radiation in the forward direction. This mechanism, leading to a dramatic violation of diffractive QCD factorization, is under consideration in the present paper. The breakdown of the diffractive (Ingelman-Schlein) QCD factorization is a result of the interplay between the soft and hard interactions, which considerably affects the corresponding observables [15]. Recently, such an effect has been analyzed in the diffractive Drell-Yan (DY) process [15,16], and here we extend our study of this interesting phenomenon to a more general case—the diffractive gauge boson production.

II. DIFFRACTIVE GAUGE BOSON PRODUCTION AMPLITUDE

Consider first the general formalism for diffractive radiation of the electroweak gauge bosons, γ^*, Z^0, and $W^\pm$, within the color dipole approach. Let us start with consideration of the distribution functions for the Fock states contributing to heavy gauge boson radiation by a quark (valence or sea) in the projectile proton.

A. Gauge boson radiation by a quark

The $q_f \to q_f\gamma^*$ transition amplitude is given by the vector $\gamma^* q$ coupling only, i.e.,

$$T(q_f \to q_f\gamma^*) = -ieZ_q\varepsilon^\mu_{\lambda_{\gamma^*}}\bar{u}_f\gamma_\mu u_f, \tag{2.1}$$

where Z_f is the quark charge and $\bar{u}_f$ and u_f are spinors for the quark of the flavor f in the final and initial states, respectively.

The couplings of Z^0 and $W^\pm$ bosons to quarks contain both vector and axial-vector parts. The $q_f \to q_f Z^0$ transition amplitude is given by

$$T(q_f \to q_f Z^0) = \frac{-ie}{\sin 2\theta_W}\varepsilon^\mu_{\lambda_Z}\bar{u}_f[g^Z_{v,f}\gamma_\mu - g^Z_{a,f}\gamma_\mu\gamma_5]u_f, \tag{2.2}$$

while the $q_f \to q_{f'}W^\pm$ amplitudes read

$$\begin{aligned} T(q_{f_u} \to q_{f_d}W^+) &= \frac{-ie}{2\sqrt{2}\sin\theta_W}V_{f_uf_d}\varepsilon^\mu_{\lambda_W}\bar{u}_{f_u}[g^W_{v,f}\gamma_\mu - g^W_{a,f}\gamma_\mu\gamma_5]u_{f_d}, \\ T(q_{f_d} \to q_{f_u}W^-) &= \frac{-ie}{2\sqrt{2}\sin\theta_W}V_{f_df_u}\varepsilon^\mu_{\lambda_W}\bar{u}_{f_d}[g^W_{v,f}\gamma_\mu - g^W_{a,f}\gamma_\mu\gamma_5]u_{f_u}, \end{aligned} \tag{2.3}$$

for the *up* ($f_u = u, c, t$) and *down* ($f_d = d, s, b$) quarks, respectively. Here, $V_{f_uf_d}$ is the Cabibbo-Kobayashi-Maskawa matrix element corresponding to $f_u \to f_d$ transition, and θ_W is the Weinberg angle. The weak mixing parameter $\sin^2\theta_W$ is related at the tree level to G_F, M_Z, and $\alpha_{\rm em}$ by $\sin^2\theta_W = 4\pi\alpha_{\rm em}/\sqrt{2}G_FM_Z^2$ [we adopt here $\alpha_{\rm em}(m_Z) \simeq 1/127.934$]. The vector couplings at the tree level are

$$g^Z_{v,f_u} = \frac{1}{2} - \frac{4}{3}\sin^2\theta_W, \quad g^Z_{v,f_d} = -\frac{1}{2} + \frac{2}{3}\sin^2\theta_W, \quad g^W_{v,f} = 1; \tag{2.4}$$

whereas axial-vector couplings are

$$g^Z_{a,f_u} = \frac{1}{2}, \qquad g^Z_{a,f_d} = -\frac{1}{2}, \qquad g^W_{a,f} = 1. \tag{2.5}$$

Heavy gauge boson polarization vectors describing transverse (T), $\lambda_G = \pm 1$, and longitudinal (L), $\lambda_G = 0$, polarization states are defined in light-cone coordinates[1] as

$$\varepsilon_{\lambda=\pm} = (0, 0, \vec{\varepsilon}_{\lambda=\pm}), \qquad \vec{\varepsilon}_{\lambda=\pm} = \mp\frac{1}{\sqrt{2}}(1, \pm i), \tag{2.6}$$

$$\varepsilon_{\lambda=0} = \left(\frac{q^+}{M}, -\frac{M}{q^+}, \vec{0}\right). \tag{2.7}$$

Note that we work in the physical (unitary) gauge. The calculations are performed in the high energy limit, i.e., in the limit where q^+ is much larger than all other scales.

Let us start with the radiation of a heavy gauge boson by a quark interacting with a proton target. We assume that the longitudinal momentum of the projectile is not changed significantly by the soft interaction at high energies. In the high energy limit the corresponding s- and u-channel amplitudes of the gauge boson bremsstrahlung in the quark-target scattering can be written as follows (cf. diffractive DY amplitude in Ref. [16]):

$$\begin{aligned} \mathcal{M}_s &\simeq -i\sqrt{4\pi}\mathcal{C}_q^G\alpha(1-\alpha)\varepsilon^\mu_\lambda\sum_\sigma\frac{\bar{u}_{\sigma_2}(p_2)[g^G_{v,f}\gamma_\mu - g^G_{a,f}\gamma_\mu\gamma_5]u_\sigma(p_2+q)}{\alpha^2l_\perp^2 + \eta^2}\mathcal{A}_{\sigma\sigma_1}(k_\perp), \\ \mathcal{M}_u &\simeq i\sqrt{4\pi}\mathcal{C}_q^G\alpha\varepsilon^\mu_\lambda\sum_\sigma\frac{\bar{u}_\sigma(p_1-q)[g^G_{v,f}\gamma_\mu - g^G_{a,f}\gamma_\mu\gamma_5]u_{\sigma_1}(p_1)}{\alpha^2(\vec{l}_\perp + \vec{k}_\perp)^2 + \eta^2}\mathcal{A}_{\sigma\sigma_2}(k_\perp), \end{aligned} \tag{2.8}$$

[1]As usual, the light-cone 4-vector p is defined as $p = (p^+, p^-, \vec{p})$, where $p^\pm = p^0 \pm p^z$.

where $G = \gamma, W^{\pm}, Z$ is the gauge boson under consideration; $\eta^2 = (1-\alpha)M^2 + \alpha^2 m_q^2$; and α is the fractional light-cone momentum carried by the gauge boson, which has invariant mass M. The vector (v) and axial-vector (a) couplings $g^{Z,W}_{v/a,f}$ are defined in Eqs. (2.4) and (2.5), whereas our notations imply $g^{\gamma}_{v,f} = 1$ and $g^{\gamma}_{a,f} = 0$; $\sigma_{1,2}$ are the helicities of initial and final quarks, respectively; $\vec{k}_\perp = \vec{p}_{2\perp} - \vec{p}_{1\perp} + \vec{q}_\perp$ is the transverse momentum of the exchanged gluon; and $\vec{l}_\perp = \vec{p}_{2\perp} - (1-\alpha)\vec{q}_\perp/\alpha$ is the transverse momentum of the final quark in the frame, where the z axis is parallel to the gauge boson momentum. The amplitude $\mathcal{A}$ for scattering of the quark on the nucleon in the target rest frame has the following approximate form [17]:

$$\mathcal{A}_{\sigma\sigma_1}(\vec{k}_\perp) \simeq 2p_1^0 \delta_{\sigma\sigma_1} \mathcal{V}_q(\vec{k}_\perp),$$
$$\mathcal{A}_{\sigma\sigma_2}(\vec{k}_\perp) \simeq 2p_2^0 \delta_{\sigma\sigma_2} \mathcal{V}_q(\vec{k}_\perp),$$

where the factorized universal amplitude $\mathcal{V}_q(\vec{k}_\perp)$ does not depend on the energy and helicity state of the quark. The coupling factor $\mathcal{C}_f^G$, $f = q, l$, introduced in Eq. (2.8), is defined for $G = \gamma^*, Z^0$, and $W^{\pm}$ bosons, respectively, as

$$\mathcal{C}_f^{\gamma} = \sqrt{\alpha_{\rm em}} Z_f, \qquad \mathcal{C}_f^{Z} = \frac{\sqrt{\alpha_{\rm em}}}{\sin 2\theta_W},$$
$$\mathcal{C}_f^{W^+} = \frac{\sqrt{\alpha_{\rm em}}}{2\sqrt{2}\sin\theta_W} V_{f_u f_d}, \qquad \mathcal{C}_f^{W^-} = \frac{\sqrt{\alpha_{\rm em}}}{2\sqrt{2}\sin\theta_W} V_{f_d f_u},$$

where $\alpha_{\rm em} = e^2/(4\pi) = 1/137$ is the electromagnetic coupling constant. In the case of gauge boson couplings to leptons, we should substitute $V_{f_u f_d} = V_{f_d f_u} = 1$.

Eventually, we can switch to impact parameter space by performing the Fourier transformation over $\vec{l}_\perp$ and $\vec{k}_\perp$ and write down the total amplitude M_q for gauge boson radiation in quark-proton scattering as follows:

$$M_q^{\mu}(\vec{b},\vec{r}) = -2ip_1^0\sqrt{4\pi}\frac{\sqrt{1-\alpha}}{\alpha^2} \times \Psi^{\mu}_{V-A}(\vec{r},\alpha,M)\cdot[V_q(\vec{b}) - V_q(\vec{b}+\alpha\vec{r})],$$
$$V_q(\vec{b}) = \int \frac{d^2k_\perp}{(2\pi)^2} e^{-i\vec{k}_\perp\cdot\vec{b}} \mathcal{V}_q(\vec{k}_\perp),$$
$$\Psi^{Z,W}_{V-A}(\vec{r},\alpha,M) = \Psi^{Z,W}_{V}(\vec{r},\alpha,M) - \Psi^{Z,W}_{A}(\vec{r},\alpha,M),$$

where $\alpha\vec{r}$ is the transverse separation between the initial and final quarks; and $\Psi^{\mu}_{V/A}(\vec{r},\alpha,M)$ are the light-cone distribution functions of the vector $q \to Vq$ and axial-vector $q \to Aq$ transitions in the mixed representation defined as

$$\Psi^{\mu}_{V}(\vec{r},\alpha,M) = \mathcal{C}_q^G g^G_{v,q}\alpha^3\sqrt{1-\alpha} \times \int \frac{d^2l_\perp}{(2\pi)^2} e^{-i\vec{l}_\perp\cdot\alpha\vec{r}} \frac{\bar{u}_{\sigma_2}(p_f)\gamma^{\mu}u_{\sigma}(p_2+q)}{\alpha^2 l_\perp^2 + \eta^2},$$
$$\Psi^{\mu}_{A}(\vec{r},\alpha,M) = \mathcal{C}_q^G g^G_{a,q}\alpha^3\sqrt{1-\alpha} \times \int \frac{d^2l_\perp}{(2\pi)^2} e^{-i\vec{l}_\perp\cdot\alpha\vec{r}} \frac{\bar{u}_{\sigma_2}(p_2)\gamma^{\mu}\gamma_5 u_{\sigma}(p_2+q)}{\alpha^2 l_\perp^2 + \eta^2}.$$

For an unpolarized initial quark the interference terms between the vector and axial-vector wave functions cancel each other, i.e.,

$$\sum_{\sigma_1,\sigma_2} \Psi^{\lambda}_{V-A}(\alpha,\vec{\rho}_1)\Psi^{\lambda *}_{V-A}(\alpha,\vec{\rho}_2) = \Psi^{\lambda}_{V}(\alpha,\vec{\rho}_1)\Psi^{\lambda *}_{V}(\alpha,\vec{\rho}_2) + \Psi^{\lambda}_{A}(\alpha,\vec{\rho}_1)\Psi^{\lambda *}_{A}(\alpha,\vec{\rho}_2). \quad (2.9)$$

The bilinear combinations of the vector V and axial-vector A light-cone distribution functions, corresponding to radiation of longitudinally ($\lambda = 0$) and transversely ($\lambda = \pm 1$) polarized gauge bosons, have the form[2]

$$\Psi^{T}_{V}(\alpha,\vec{\rho}_1)\Psi^{T *}_{V}(\alpha,\vec{\rho}_2) = \sum_{\lambda=\pm1}\frac{1}{2}\sum_{\sigma_1,\sigma_2}\epsilon^*_{\mu}(\lambda)\Psi^{\mu}_{V}(\alpha,\vec{\rho}_1)\epsilon_{\nu}(\lambda)\Psi^{\nu *}_{V}(\alpha,\vec{\rho}_2)$$
$$= \frac{\mathcal{C}_q^2 (g^G_{v,q})^2}{2\pi^2}\Big\{m_q^2\alpha^4 \mathrm{K}_0(\eta\rho_1)\mathrm{K}_0(\eta\rho_2) + [1+(1-\alpha)^2]\eta^2\frac{\vec{\rho}_1\cdot\vec{\rho}_2}{\rho_1\rho_2}\mathrm{K}_1(\eta\rho_1)\mathrm{K}_1(\eta\rho_2)\Big\},$$
$$\Psi^{L}_{V}(\alpha,\vec{\rho}_1)\Psi^{L *}_{V}(\alpha,\vec{\rho}_2) = \frac{1}{2}\sum_{\sigma_1,\sigma_2}\epsilon^*_{\mu}(\lambda=0)\Psi^{\mu}_{V}(\alpha,\vec{\rho}_1)\epsilon_{\nu}(\lambda=0)\Psi^{\nu *}_{V}(\alpha,\vec{\rho}_2)$$
$$= \frac{\mathcal{C}_q^2 (g^G_{v,q})^2}{\pi^2} M^2(1-\alpha)^2 \mathrm{K}_0(\eta\rho_1)\mathrm{K}_0(\eta\rho_2). \quad (2.10)$$

$$\Psi^{T}_{A}(\alpha,\vec{\rho}_1)\Psi^{T *}_{A}(\alpha,\vec{\rho}_2) = \frac{\mathcal{C}_q^2 (g^G_{a,q})^2}{2\pi^2}\Big\{m_q^2\alpha^2(2-\alpha)^2 \mathrm{K}_0(\eta\rho_1)\mathrm{K}_0(\eta\rho_2) + [1+(1-\alpha)^2]\eta^2\frac{\vec{\rho}_1\cdot\vec{\rho}_2}{\rho_1\rho_2}\mathrm{K}_1(\eta\rho_1)\mathrm{K}_1(\eta\rho_2)\Big\},$$
$$\Psi^{L}_{A}(\alpha,\vec{\rho}_1)\Psi^{L *}_{A}(\alpha,\vec{\rho}_2) = \frac{\mathcal{C}_q^2 (g^G_{a,q})^2}{\pi^2}\frac{\eta^2}{M^2}\Big\{\eta^2 \mathrm{K}_0(\eta\rho_1)\mathrm{K}_0(\eta\rho_2) + \alpha^2 m_q^2\frac{\vec{\rho}_1\cdot\vec{\rho}_2}{\rho_1\rho_2}\mathrm{K}_1(\eta\rho_1)\mathrm{K}_1(\eta\rho_2)\Big\}, \quad (2.11)$$

where the averaging over helicity of the initial quark is performed.

[2]In the case of a heavy photon γ^* bremsstrahlung by a quark, such formulas were derived in Refs. [17–19].

B. Forward diffractive radiation from a dipole

The amplitude of diffractive gauge boson radiation by a quark-antiquark dipole does not vanish in the forward direction, unlike the radiation by a single quark [13,15]. This can be understood as follows. According to the general theory of diffraction [1–4], the off-diagonal diffractive channels are possible only if different Fock components of the projectile (eigenstates of interaction) interact with different elastic amplitudes. Clearly, the two Fock states consisting of just a quark and of a quark plus a gauge boson interact equally, if their elastic amplitudes are integrated over impact parameter. Indeed, when a quark fluctuates into a state $|qG\rangle$ containing the gauge boson G, with the transverse quark-boson separation $\vec{r}$, the quark gets a transverse shift $\Delta\vec{r} = \alpha\vec{r}$. The impact parameter integration gives the forward amplitude. Both Fock states $|q\rangle$ and $|qG\rangle$ interact with the target with the same total cross section; this is why a quark cannot radiate at zero momentum transfer, and, hence, G is not produced diffractively in the forward direction. This is the general and model-independent statement. The details of this general consideration can be found in Ref. [13] (Appendixes A1 and A4). The same result is obtained by calculating Feynman graphs in Appendix B4 of the same paper. The unimportance of radiation between two interactions was also demonstrated by Brodsky and Hoyer in Ref. [20].

Notice that in all these calculations one assumes that the coherence time of radiation considerably exceeds the time interval between the two interactions, which is fulfilled in our case, since we consider radiation at forward rapidities.

The situation changes if the boson is radiated diffractively by a dipole. Then the quark dipoles with or without a gauge boson have different sizes and interact with the target differently. So the amplitude of the diffractive gauge boson radiation from the $q\bar{q}$ dipole is proportional to the difference between elastic amplitudes of the two Fock components, $|q\bar{q}\rangle$ and $|q\bar{q}G\rangle$ [15], i.e.,

$$M_{\bar{q}q}(\vec{b},\vec{r}_p,\vec{r},\alpha) = -2ip_1^0\sqrt{4\pi}\frac{\sqrt{1-\alpha}}{\alpha^2}\Psi^{\mu}_{\gamma^* q}(\alpha,\vec{r})[2\mathrm{Im}f_{\mathrm{el}}(\vec{b},\vec{r}_p) - 2\mathrm{Im}f_{\mathrm{el}}(\vec{b},\vec{r}_p+\alpha\vec{r})], \quad (2.12)$$

where $\vec{r}_p$ is the transverse separation of the $q\bar{q}$ dipole. The partial elastic dipole-proton amplitude is normalized to the dipole cross section, which is parameterized by the following simple ansatz [21]:

$$\sigma_{\bar{q}q}(r_p,x) = \int d^2b 2\mathrm{Im}f_{\mathrm{el}}(\vec{b},\vec{r}_p) = \sigma_0(1-e^{-r_p^2/R_0^2(x)}), \quad (2.13)$$

where $\sigma_0 = 23.03$ mb, $R_0(x) = 0.4$ fm $\times (x/x_0)^{0.144}$, and $x_0 = 0.003$. This saturated form, although oversimplified (compare with Ref. [22]), is rather successful in the description of experimental HERA data with a reasonable accuracy. We rely on this parametrization in what follows, and the explicit form of the amplitude $f_{\mathrm{el}}(\vec{b},\vec{r})$ will be specified later.

The diffractive amplitude (2.12), thus, occurs to be sensitive to the large transverse separations between the projectile quarks in the incoming proton. These distances are controlled by a nonperturbative scale, which is one of the reasons for the breakdown of diffractive QCD factorization in the diffractive gauge boson production (for more details, see Refs. [15,16]).

III. SINGLE DIFFRACTIVE CROSS SECTION

The differential cross section for the single diffractive dilepton ($l\bar{l}$ pair in the case of γ^* and Z and $l\nu_l$ pair in the case of $W^{\pm}$) production in the target rest frame can be written in terms of the gauge boson production cross section at a given invariant mass of the dilepton M. Integrating the cross section over the solid angle of the lepton pair and the boson transverse momentum $\vec{q}_\perp$, we get for the diffractive Drell-Yan cross section [16]

$$\frac{d^6\sigma_{L,T}(pp\to pl\bar{l}X)}{d^2q_\perp dx_1 dM^2 d^2\delta_\perp} = \frac{\alpha_{\mathrm{em}}}{3\pi M^2}\frac{d^5\sigma_{L,T}(pp\to p\gamma^* X)}{d^2q_\perp dx_1 d^2\delta_\perp}, \quad (3.1)$$

where x_1 is the fractional light-cone momentum of the dilepton, $\vec{\delta}_\perp$ is the transverse momentum of the recoil proton, and $\vec{q}_\perp$ is the transverse momentum of the outgoing photon (or dilepton). Compared to our previous study, here we are going to look at the $q_\perp$ dependence of the diffractive DY cross section in a much wider range of dilepton invariant masses accessible at the LHC.

In the case of the diffractive production of $G = Z^0, W^{\pm}$ bosons, it is convenient to employ the simple and phenomenologically successful model for the invariant mass distribution in the decay of an unstable particle (for details, see, e.g., Ref. [23]) and to present the differential cross section in the factorized form

$$\frac{d^4\sigma_{L,T}(pp\to p(G^*\to l\bar{l},l\bar{\nu}_l)X)}{d^2q_\perp dx_1 dM^2 d^2\delta_\perp} = \mathrm{Br}(G\to l\bar{l},l\nu_l)\rho_G(M)\frac{d^3\sigma_{L,T}(pp\to pG^*X)}{d^2q_\perp dx_1 d^2\delta_\perp}, \quad (3.2)$$

where $\mathrm{Br}(Z^0\to\sum_{l=e,\mu,\tau}l\bar{l})\simeq 0.101$ and $\mathrm{Br}(W^{\pm}\to\sum_{l=e,\mu,\tau}l\nu_l)\simeq 0.326$ [24] are the leptonic branching ratios of Z^0 and $W^{\pm}$ bosons, respectively, and $\rho_G(M)$ is the invariant mass distribution of the dileptons from the decay of the gauge boson G:

$$\rho_G(M) = \frac{1}{\pi}\frac{M\Gamma_G(M)}{(M^2-m_G^2)^2+[M\Gamma_G(M)]^2}, \quad \Gamma_G(M)/M \ll 1. \quad (3.3)$$

Here, m_G is the fixed on-shell boson mass, and $\Gamma_G(M)$ is its total decay width defined in the standard way by substitution $m_G \to M$, i.e.,

$$\Gamma_W(M) \simeq \frac{3\alpha_{\rm em} M}{4\sin^2\theta_W},$$
$$\Gamma_Z(M) \simeq \frac{\alpha_{\rm em} M}{6\sin^2 2\theta_W}\left[\frac{160}{3}\sin^4\theta_W - 40\sin^2\theta_W + 21\right]. \tag{3.4}$$

Let us assume that the gauge boson is emitted by the quark q_1. As a result of the hard emission, the quark position in the impact parameters, being initially $\vec{r}_1$, gets shifted to $\vec{r}_1 + \alpha\vec{r}$. Applying the completeness relation to the wave function of the proton remnant in the final state

$$\sum_f \Psi_f(\vec{r}_1 + \alpha\vec{r}, \vec{r}_2, \vec{r}_3; \{x_q^{1,2,\cdots}\}, \{x_g^{1,2,\cdots}\})\Psi_f^*(\vec{r}_1' + \alpha\vec{r}', \vec{r}_2', \vec{r}_3'; \{x_q'^{1,2,\cdots}\}, \{x_g'^{1,2,\cdots}\})$$
$$= \delta(\vec{r}_1 - \vec{r}_1' + \alpha(\vec{r} - \vec{r}'))\delta(\vec{r}_2 - \vec{r}_2')\delta(\vec{r}_3 - \vec{r}_3')\prod_j \delta(x_{q/g}^j - x_{q/g}'^j), \tag{3.5}$$

where $\vec{r}_i$ and $x_{q/g}^i$ are the transverse coordinates and fractional light-cone momenta of the valence or sea quarks and gluons, we get the diffractive G^* production cross section in the following form [15,16]:

$$\frac{d^5\sigma_{\lambda_G}(pp \to pG^*X)}{d^2q_\perp dx_1 d^2\delta_\perp} = \frac{1}{(2\pi)^2}\frac{1}{64\pi^2}\frac{1}{x_1}\sum_{q=\rm val,sea}\int d^2r_1 d^2r_2 d^2r_3 d^2r d^2r' d^2b d^2b' dx_q \prod_i dx_q^i dx_g^i$$
$$\times \Psi_{V-A}^{\lambda_G}(\vec{r}, \alpha, M)\Psi_{V-A}^{\lambda_G *}(\vec{r}', \alpha, M)|\Psi_i(\vec{r}_1, \vec{r}_2, \vec{r}_3; x_q, \{x_q^{2,3,\cdots}\}, \{x_g^{2,3,\cdots}\})|^2$$
$$\times \Delta(\vec{r}_1, \vec{r}_2, \vec{r}_3; \vec{b}; \vec{r}, \alpha)\Delta(\vec{r}_1, \vec{r}_2, \vec{r}_3; \vec{b}'; \vec{r}', \alpha)e^{i\vec{\delta}_\perp\cdot(\vec{b}-\vec{b}')}e^{i\vec{l}_\perp\cdot\alpha(\vec{r}-\vec{r}')}, \tag{3.6}$$

where Ψ_i is the proton wave function, the summation is performed over all valence or sea quarks and gluons in the proton, and the light-cone fraction of the quark emitting the gauge boson $x_q^1 \equiv x_q$ is fixed by the external phase space variables x_1 and α due to the momentum conservation, namely,

$$x_q = \frac{x_1}{\alpha}, \qquad x_1 = \frac{q^+}{P_1^+}, \tag{3.7}$$

where P_1 is the 4-momentum of the projectile proton, q is the 4-momentum of the produced gauge boson, and

$$\Delta = -2{\rm Im}f_{\rm el}(\vec{b}, \vec{r}_1 - \vec{r}_2) + 2{\rm Im}f_{\rm el}(\vec{b}, \vec{r}_1 - \vec{r}_2 + \alpha\vec{r})$$
$$- 2{\rm Im}f_{\rm el}(\vec{b}, \vec{r}_1 - \vec{r}_3) + 2{\rm Im}f_{\rm el}(\vec{b}, \vec{r}_1 - \vec{r}_3 + \alpha\vec{r}) \tag{3.8}$$

is the properly normalized diffractive amplitude, where $f_{\rm el}(\vec{b}, \vec{r}_1 - \vec{r}_2)$ is the partial elastic amplitude for dipole of transverse size r colliding with a proton at impact parameter b to be specified below. As expected, the diffractive amplitude Δ is proportional to the difference between elastic amplitudes for the dipoles of slightly different sizes. This difference is suppressed by absorptive corrections, the effect sometimes called survival probability of large rapidity gaps.

[3]Such a statement has already been made in a similar analysis of the diffractive heavy flavor production performed in Ref. [14] and in our previous work on diffractive DY study [16].

The amplitude Eq. (3.8) is the full expression, which includes by default the effect of absorption and does not need any extra survival probability factor.[3] This can be illustrated on a simple example of elastic dipole scattering off a potential. The dipole elastic amplitude has the eikonal form

$${\rm Im}\, f_{\rm el}(\vec{b}, \vec{r}_1 - \vec{r}_2) = 1 - \exp[i\chi(\vec{r}_1) - i\chi(\vec{r}_2)], \tag{3.9}$$

where

$$\chi(b) = -\int_{-\infty}^{\infty} dz V(\vec{b}, z), \tag{3.10}$$

and $V(\vec{b}, z)$ is the potential, which depends on the impact parameter and longitudinal coordinate, and is nearly imaginary at high energies. The difference between elastic amplitudes with a shifted quark position, which enters the diffractive amplitude, reads

$${\rm Im}\, f_{\rm el}(\vec{b}, \vec{r}_1 - \vec{r}_2 + \alpha\vec{r}) - {\rm Im}f_{\rm el}(\vec{b}, \vec{r}_1 - \vec{r}_2)$$
$$= \exp[i\chi(\vec{r}_1) - i\chi(\vec{r}_2)]\exp[i\alpha\vec{r}\cdot\vec{\nabla}\chi(\vec{r}_1)]. \tag{3.11}$$

The first factor $\exp[i\chi(\vec{r}_1) - i\chi(\vec{r}_2)]$ is exactly the survival probability amplitude, which vanishes in the black-disk limit, as it should be. This proves that the cross section Eq. (3.6) includes the effect of absorption. Notice that usually the survival probability factor is introduced into the diffractive cross section probabilistically, while in

Eq. (3.6) it is treated quantum mechanically, at the amplitude level.

All the elastic amplitudes in Eq. (3.8) implicitly depend on energy. They cannot be calculated reliably but are known from phenomenology. Since large dipole sizes $|\vec{r}_i - \vec{r}_j| \sim b \sim R_p$, $i \neq j$ (R_p is the mean proton size), are important in Eq. (3.8), the Bjorken variable x is ill defined, and the collision energy is a more appropriate variable. A parametrization of the dipole cross section as a function of s was proposed and fitted to data in Ref. [13], and the corresponding partial dipole amplitude is given by [25–27]

$$\mathrm{Im} f_{\mathrm{el}}(\vec{b}, \vec{r}_p, s, x_q) = \frac{\sigma_0(s)}{8\pi\mathcal{B}(s)}\left\{\exp\left[-\frac{[\vec{b} + \vec{r}_p(1-x_q)]^2}{2\mathcal{B}(s)}\right] + \exp\left[-\frac{[\vec{b} + \vec{r}_p x_q]^2}{2\mathcal{B}(s)}\right] - 2\exp\left[-\frac{r_p^2}{R_0^2(s)} - \frac{[\vec{b} + \vec{r}_p(1/2 - x_q)]^2}{2\mathcal{B}(s)}\right]\right\},$$
$$\mathcal{B}(s) = R_N^2(s) + R_0^2(s)/8, \tag{3.12}$$

where x_q is the quark longitudinal quark fraction in the dipole defined in Eq. (3.7), and

$$R_0(s) = 0.88\ \mathrm{fm}(s_0/s)^{0.14},$$
$$R_N^2(s) = B_{\mathrm{el}}^{\pi p}(s) - \frac{1}{4}R_0^2(s) - \frac{1}{3}\langle r_{\mathrm{ch}}^2\rangle_\pi, \tag{3.13}$$
$$\sigma_0(s) = \sigma_{\mathrm{tot}}^{\pi p}(s)\left(1 + \frac{3R_0^2(s)}{8\langle r_{\mathrm{ch}}^2\rangle_\pi}\right).$$

Here, the pion-proton total cross section is parameterized as [28] $\sigma_{\mathrm{tot}}^{\pi p}(s) = 23.6(s/s_0)^{0.08}$ mb, $s_0 = 1000\ \mathrm{GeV}^2$, the mean pion radius squared is [29] $\langle r_{\mathrm{ch}}^2\rangle_\pi = 0.44\ \mathrm{fm}^2$, and the Regge parametrization of the elastic slope $B_{\mathrm{el}}^{\pi p}(s) = B_0 + 2\alpha'_{\mathbb{P}}\ln(s/\mu^2)$, with $B_0 = 6\ \mathrm{GeV}^{-2}$, $\alpha'_{\mathbb{P}} = 0.25\ \mathrm{GeV}^{-2}$, and $\mu^2 = 1\ \mathrm{GeV}^2$ can be used. We employ the s-dependent parametrization (3.12) in what follows, because diffraction is essentially controlled by soft interactions.

Finally, we parameterize the proton wave function assuming the symmetric Gaussian shape for the spacial valence quark distributions in the proton, as

$$|\Psi_i(\vec{r}_1, \vec{r}_2, \vec{r}_3; x_q, \{x_q^{2,3,\cdots}\}, \{x_g^{2,3,\cdots}\})|^2 = \frac{3a^2}{\pi^2}e^{-a(r_1^2+r_2^2+r_3^2)}\rho(x_q, \{x_q^{2,3,\cdots}\}, \{x_g^{2,3,\cdots}\}) \times \delta(\vec{r}_1 + \vec{r}_2 + \vec{r}_3)\delta\left(1 - x_q - \sum_j x_{q/g}^j\right), \tag{3.14}$$

where the sum is taken over all valence or sea quarks and gluons not participating in the hard interaction, x_q is defined in Eq. (3.7), $a = \langle r_{\mathrm{ch}}^2\rangle^{-1}$ is the inverse proton mean charge radius squared, and ρ is the valence quark distribution function in the proton. Notice that this distribution has a low scale, so the valence quarks carry the whole momentum of the proton, while gluons and the sea are included in the constituent valence quarks. The Gottfried sum rule based on this assumption is known to be broken [30], but we neglect the related $\sim$20% correction.

Integrating over the fractional momenta of all partons not participating in the hard interaction, we arrive at the single valence quark distribution in the proton, probed by the hard process—radiation of a heavy gauge boson,

$$\int\prod_i dx_q^i dx_g^i \delta\left(1 - x_q - \sum_j x_{q/g}^j\right)\rho(x_q, \{x_q^{2,3,\cdots}\}, \{x_g^{2,3,\cdots}\}) = \rho_q(x_q), \tag{3.15}$$

where q denotes the quark flavor emitting the gauge boson G with the fraction x_q given by Eq. (3.7). In the case of a diffractive Drell-Yan reaction [16], generalization of the three-body proton wave function (3.14) including different quark and antiquark flavors leads to the proton structure function as

$$\sum_q Z_q^2[\rho_q(x_q) + \rho_{\bar{q}}(x_q)] = \frac{1}{x_q}F_2(x_q). \tag{3.16}$$

However, in the case of diffractive W and Z production, the coupling factor $C_q^G g_{v/a,q}^G$ varies for different (valence or sea) quark species in the proton, so one has to deal with the original quark densities. Similar to the diffractive DY case, in actual numerical calculations below, when summing up the contributions of different quark flavors, we will generalize the above approach including the sea quark and antiquark densities in the proton at the hard scale imposed by the mass of the gauge boson. Also, the interference terms between amplitudes corresponding to gauge boson radiated by different valence quarks separated by large transverse distances in the proton are strongly suppressed in the hard limit $r \ll R_0(s)$ and are neglected.

IV. SINGLE DIFFRACTIVE CROSS SECTION IN THE FORWARD LIMIT

A. The two-scale approximation

The typical hard length scale related to hard vector boson production, $\alpha r \sim \alpha/(1-\alpha)M$, is usually much smaller than any hadronic scale (see, however, the next

section). Relying on the smallness of the hard scale, $\alpha r \ll R_{ij} = |\vec{r}_i - \vec{r}_j| \sim R_p$, one can derive an approximate analytical formula for the diffractive cross section (3.6):

$$\mathrm{Im}\, f_{\mathrm{el}}(\vec{b}, \vec{R}_{ij} + \alpha\vec{r}) - \mathrm{Im} f_{\mathrm{el}}(\vec{b}, \vec{R}_{ij}) \simeq \frac{\partial \mathrm{Im} f_{\mathrm{el}}(\vec{b}, \vec{R}_{ij})}{\partial \vec{R}_{ij}} \alpha\vec{r}. \tag{4.1}$$

For the sake of convenience, we modify the integrals in Eq. (3.6) by introducing new variables $\vec{r}_2 \to \vec{R}_{12}$ and $\vec{r}_3 \to \vec{R}_{13}$, so that

$$\int d^2r_1 d^2r_2 d^2r_3 e^{-a(r_1^2+r_2^2+r_3^2)} \delta(\vec{r}_1 + \vec{r}_2 + \vec{r}_3) = \frac{1}{9} \int d^2R_{12} d^2R_{13} e^{-\frac{2a}{3}(R_{12}^2 + R_{13}^2 + \vec{R}_{12}\vec{R}_{13})}. \tag{4.2}$$

Since in the forward limit $\delta_\perp \to 0$ the b dependence comes only into the partial dipole amplitude f_{el} defined in Eq. (3.12), it can be easily integrated [15]:

$$\int d^2b \frac{\partial \mathrm{Im} f_{\mathrm{el}}(\vec{b}, \vec{R}_{ij})}{\partial \vec{R}_{ij}} = \frac{\sigma_0(s)}{R_0^2(s)} \vec{R}_{ij} e^{-R_{ij}^2/R_0^2(s)}, \tag{4.3}$$

with the energy-dependent parameters defined after Eq. (3.12).

We see that the amplitude of diffractive gauge boson emission in the dipole-target scattering (2.12) integrated over $\vec{b}$,

$$\int d^2b M_{qq}(\vec{b}, \vec{R}_{ij}, \vec{r}, \alpha) \propto \alpha \frac{\sigma_0(s)}{R_0^2(s)} (\vec{r} \cdot \vec{R}_{ij}) e^{-R_{ij}^2/R_0^2(s)}, \tag{4.4}$$

is proportional to the product of the hard scale $r \sim 1/(1-\alpha)M$ and the soft hadronic scale $R_{ij} \sim R_0 \sim 1/\Lambda_{\mathrm{QCD}}$. This means that the single diffractive cross section depends on the hard scale as $\sigma_{\mathrm{sd}} \sim r^2 \sim 1/M^2$.

It is well known that the cross section of diffractive deep inelastic scattering (DDIS) $\sigma_{\mathrm{DDIS}} \sim r^4$ is dominated essentially by soft fluctuations at large r (for more details, see, e.g., Ref. [5]), as correctly predicted by the diffractive (Ingelman-Schlein) QCD factorization. This happens since the end-point $q\bar{q}$ dipole fluctuations, driving the cross section at $\alpha \to 0$ or 1, have no hard scale dependence for light quarks $m_q \ll Q^2$. In this case, the Q^2 dependence comes only into their weight as $\sim 1/Q^2$, even though it is of the higher twist nature.

In opposition, the single diffractive gauge bosons production cross section behaves as $\sim \vec{r} \cdot \vec{R}$, soft and hard fluctuations contribute in this process on the same footing, and their interplay does not depend on the hard scale, similar to the inclusive gauge boson production. Hence, the forward diffractive Abelian radiation turns out to be of the leading twist nature, and the diffractive-to-inclusive production cross sections ratio can depend on the hard scale only weakly through the x dependence of the saturation scale, or more precisely $R_0(x_2)$, and can only increase (see below).

However, if one uses the conventional diffractive factorization scheme [7] the single diffractive cross section, similarly to the DDIS process, one does not find any soft-hard interplay as observed above, and the cross section turns out to behave as $\sim r^4$, providing the higher twist nature of the single diffractive process. Correspondingly, this strongly affects the M^2 dependence of the diffractive-to-inclusive boson production cross section ratio, such that it decreases with M^2, opposite to our observation above.

Therefore, the fundamental interplay between the hard and soft interactions in the forward diffractive Abelian radiation is *the major reason for the diffractive QCD factorization breaking* leading to quite unusual features of the corresponding observables (for a similar discussion in the diffractive DY, see Refs. [15,16]). As we have emphasized above, this interplay is absent in the DDIS and in diffractive QCD factorization-based approaches to the diffractive DY (see, e.g., Ref. [11]) leading to the energy and scale dependence of the corresponding cross section which is completely opposite to the one predicted above by the color dipole model.

Furthermore, the integrations over $\vec{R}_{12}$ and $\vec{R}_{13}$ can be performed analytically leading to the diffractive cross section (3.6) in the forward limit $\delta_\perp \to 0$:

$$\frac{d^4\sigma_{\lambda_G}(pp \to pG^*X)}{d^2q_\perp dx_1 d\delta_\perp^2}\Big|_{\delta_\perp=0} = \frac{a^2}{24\pi^3} \frac{\sigma_0^2(s)}{R_0^4(s)} \frac{1}{A_2} \left[\frac{2}{(A_2-4A_1)^2} + \frac{A_2^2}{(A_2^2-4A_3^2)^2}\right] \times \sum_q \int_{x_1}^1 d\alpha \left[\rho_q\left(\frac{x_1}{\alpha}\right) + \rho_{\bar{q}}\left(\frac{x_1}{\alpha}\right)\right] \int d^2r d^2r' (\vec{r}\cdot\vec{r}') \Psi_{V-A}^{\lambda_G}(\vec{r}, \alpha, M) \Psi_{V-A}^{\lambda_G *}(\vec{r}', \alpha, M) e^{i\vec{q}_\perp \cdot (\vec{r}-\vec{r}')}, \tag{4.5}$$

where

$$A_1 = \frac{2a}{3} + \frac{2}{R_0^2(s)}, \qquad A_2 = \frac{2a}{3}, \qquad A_3 = \frac{2a}{3} + \frac{1}{R_0^2(s)}. \tag{4.6}$$

Assuming Gaussian $\delta_\perp$ dependence of the cross section, the $\delta_\perp$ integrated and forward cross sections are related as

$$\frac{d\sigma(pp \to pG^*X)}{d^2q_\perp dx_1} = \frac{1}{B_{\rm sd}(s)} \frac{d^3\sigma(pp \to pG^*X)}{d^2q_\perp dx_1 d\delta_\perp^2}\Big|_{\delta_\perp=0}. \tag{4.7}$$

The slope of the single diffractive cross section, $B_{\rm sd}(s) \simeq \langle r_{\rm ch}^2\rangle/3 + 2\alpha'_{\mathbb{P}} \ln(s/s_0)$, is similar to the one measured in diffractive DIS. In the next section, we will explicitly derive the diffractive slope from the explicit parameterization for the partial dipole amplitude (3.12).

Finally, one can explicitly calculate the remaining integrations in the transverse plane over $\vec{r}$ and $\vec{r}'$ by means of the following Fourier transforms:

$$\begin{aligned} J_1(q_\perp, \eta) &\equiv \int d^2r d^2r' (\vec{r}\cdot\vec{r}') K_0(\eta r) K_0(\eta r') e^{i\vec{q}_\perp\cdot(\vec{r}-\vec{r}')} \\ &= 16\pi^2 \frac{q_\perp^2}{(\eta^2+q_\perp^2)^4}, \\ J_2(q_\perp, \eta) &\equiv \int d^2r d^2r' \frac{(\vec{r}\cdot\vec{r}')^2}{rr'} K_1(\eta r) K_1(\eta r') e^{i\vec{q}_\perp\cdot(\vec{r}-\vec{r}')} \\ &= 8\pi^2 \frac{\eta^4+q_\perp^4}{\eta^2(\eta^2+q_\perp^2)^4}. \end{aligned} \tag{4.8}$$

And we arrive at the following expressions for the cross section of transversely and longitudinally polarized gauge boson production, respectively:

$$\begin{aligned} \frac{d^4\sigma_T(pp \to pG^*X)}{d^2q_\perp dx_1} &= \frac{1}{B_{\rm sd}(s)} \frac{a^2}{24\pi^3} \frac{\sigma_0^2(s)}{R_0^4(s)} \frac{1}{A_2}\left[\frac{2}{(A_2-4A_1)^2} + \frac{A_2^2}{(A_2^2-4A_3^2)^2}\right] \sum_q \frac{(\mathcal{C}_q^G)^2}{2\pi^2} \int_{x_1}^1 d\alpha \left[\rho_q\left(\frac{x_1}{\alpha}\right) + \rho_{\bar{q}}\left(\frac{x_1}{\alpha}\right)\right] \\ &\times \{m_q^2\alpha^2[(g_{v,q}^G)^2\alpha^2 + (g_{a,q}^G)^2(2-\alpha)^2]J_1 + [(g_{v,q}^G)^2 + (g_{a,q}^G)^2][1+(1-\alpha)^2]\eta^2 J_2\}; \end{aligned} \tag{4.9}$$

$$\begin{aligned} \frac{d^4\sigma_L(pp \to pG^*X)}{d^2q_\perp dx_1} &= \frac{1}{B_{\rm sd}(s)} \frac{a^2}{24\pi^3} \frac{\sigma_0^2(s)}{R_0^4(s)} \frac{1}{A_2}\left[\frac{2}{(A_2-4A_1)^2} + \frac{A_2^2}{(A_2^2-4A_3^2)^2}\right] \sum_q \frac{(\mathcal{C}_q^G)^2}{\pi^2} \int_{x_1}^1 d\alpha \left[\rho_q\left(\frac{x_1}{\alpha}\right) + \rho_{\bar{q}}\left(\frac{x_1}{\alpha}\right)\right] \\ &\times \left\{\left[(g_{v,q}^G)^2 M^2(1-\alpha)^2 + (g_{a,q}^G)^2 \frac{\eta^4}{M^2}\right]J_1 + (g_{a,q}^G)^2\alpha^2 m_q^2 \frac{\eta^2}{M^2} J_2\right\}. \end{aligned} \tag{4.10}$$

These expressions for the differential distributions in the transverse momentum of the produced gauge bosons allow us to perform $\vec{q}_\perp$ integration via the substitution

$$\begin{aligned} J_1(q_\perp, \eta) \to I_1(\eta) &\equiv \int d^2q_\perp J_1(q_\perp, \eta) = \frac{8\pi^3}{3\eta^4}, \\ J_2(q_\perp, \eta) \to I_2(\eta) &\equiv \int d^2q_\perp J_2(q_\perp, \eta) = \frac{16\pi^3}{3\eta^4}. \end{aligned}$$

The rest of the integrations over α and x_1 can be done numerically.

B. Asymptotic behavior of diffraction

In most of theoretical models, the partial elastic amplitude of hadron scattering is expected to reach the Froissart regime, which corresponds to saturation of unitarity for the amplitudes of all Fock states within a disk in the impact parameter plane, with the radius rising as $\ln s$. In this case, diffraction vanishes everywhere, except the periphery of the disk, so the the fraction of diffractive cross section is expected to fall with energy as $\sigma_{\rm diff}/\sigma_{\rm tot} \propto 1/\ln s$ [4].

However, Eqs. (4.5) and (4.6) at $s \to \infty$, when $R_0(s) \to 0$, lead to the forward diffractive cross section proportional to $\sigma_{\rm tot}^2(s)$. So the b-integrated diffractive cross section behaves like the elastic and total cross sections, contrary to the above expectations.

To trace the origin of this problem, we should recheck our starting assumptions. So far, we assumed that the hard length scale $r \sim 1/M$, which is indeed tiny, is much smaller than any other soft hadronic scale. However, the hierarchy of scales is expected to change at asymptotically high energies. This is related to the rising energy dependence of the saturation scale in the proton, $Q_s = 1/R_0(s) = 0.086\ \text{GeV} \times (s/1\ \text{GeV}^2)^{0.14}$, where we rely on the parametrization Eq. (3.13). Although this power energy dependence is rather steep, the saturation scale reaches the gauge boson mass at the energy $s \approx 3 \times 10^9\ \text{GeV}^2$, which is much higher than that of the LHC. Therefore, in the energy range of LHC the hard length scale $\sim 1/M$ remains the shortest in the process, and the expansion Eq. (4.1) can be employed. Indeed, we performed an exact numerical calculation of the cross section Eq. (3.6) and found no sizable deviation from Eq. (4.5).

Apparently, the root of the problem is the approximation of $1/M \ll R_0(s)$, which breaks at very large s. To demonstrate analytically that the fractional diffractive cross section (3.6) vanishes at asymptotic energies, let us consider a simple example of radiation of a heavy gauge boson by a dipole of size R. In this case, the forward diffractive amplitude, i.e., the amplitude Eq. (3.8) integrated over b, takes the form ($\alpha = 1$)

$$\begin{aligned} A(\vec{R}, \vec{r}, s, \delta_\perp = 0) &= \sigma_{\bar{q}q}(\vec{R}+\vec{r}, s) - \sigma_{\bar{q}q}(\vec{R}, s) \\ &= \sigma_0(s)[e^{-R^2/R_0^2(s)} - e^{-(\vec{R}+\vec{r})^2/R_0^2(s)}]. \end{aligned} \tag{4.11}$$

This amplitude should be averaged over the R and r distributions:

$$\begin{aligned}A(s,\delta_\perp=0)&=\int d^2Rd^2r|\Psi_h(R)|^2|\Psi_{qG}(r)|^2\Delta(\vec{R},\vec{r},s)\\&=\pi R_0^2(s)\sigma_0(s)\Big[|\Psi_h(0)|^2\\&\quad-\int d^2r|\Psi_h(r)|^2|\Psi_{qG}(r)|^2\Big]\\&=R_0^2(s)\frac{\sigma_0(s)\langle r^2\rangle/\langle R^2\rangle}{\langle R^2\rangle+\langle r^2\rangle}\\&\approx R_0^2(s)\sigma_0(s)\frac{\langle r^2\rangle}{\langle R^2\rangle^2}.\end{aligned}\tag{4.12}$$

Here we assumed the energy to be sufficiently high, so $R_0(s)\to 0$ and $R_0^2(s)\ll\langle r^2\rangle$. We also assumed that the distribution function of the dipole $\Psi_h(R)$ and of the $q-G$ fluctuation $\Psi_{qG}(r)$ have Gaussian form with averaged values $\langle R^2\rangle$ and $\langle r^2\rangle$, respectively.

According to the parametrization (3.13), the ratio of forward diffractive amplitude Eq. (4.12) to the forward elastic amplitude vanishes as

$$\frac{A(s,\delta_\perp=0)}{A_{\rm el}(s,\delta_\perp=0)}\approx R_0^2(s)\frac{2\langle r^2\rangle}{\langle R^2\rangle^2}\propto s^{-0.28}.\tag{4.13}$$

In fact, the parametrization (3.13) fitted to available data is not expected to be valid at asymptotically high energies. The saturation scale corresponding to a transition from the linear Balitsky-Fadin-Kuraev-Lipatov evolution at $Q>Q_s$ to the nonlinear saturation regime at $Q<Q_s$ rises with energy as $Q_s=1/R_0(s)\propto\exp[\text{const}\times\sqrt{\ln s}]$ [31]. So it is steeply falling with energy, also slower than in (4.13).

Thus, the diffractive amplitude vanishes at very high, currently unreachable energies, while within the available energy range the expression (4.5) is sufficiently accurate.

V. DIFFRACTIVE VS INCLUSIVE PRODUCTION OF GAUGE BOSONS

The dipole description of inclusive gauge boson production can be obtained by generalizing what is known for the inclusive Drell-Yan process [18,19,32]. The cross section of inclusive production of a virtual gauge boson G^* with mass M and transverse momentum $q_\perp$ has the form

$$\begin{aligned}\frac{d^4\sigma_{\lambda_G}(pp\to G^*X)}{d^2q_\perp dx_1}&=\frac{1}{(2\pi)^2}\sum_q\int_{x_1}^1\frac{d\alpha}{\alpha^2}\Big[\rho_q\Big(\frac{x_1}{\alpha}\Big)+\rho_{\bar q}\Big(\frac{x_1}{\alpha}\Big)\Big]\int d^2rd^2r'\frac{1}{2}\{\sigma(\alpha r)+\sigma(\alpha r')-\sigma(\alpha|\vec r-\vec r'|)\}\\&\quad\times\Psi_{V-A}^{\lambda_G}(\vec r,\alpha,M)\Psi_{V-A}^{\lambda_G*}(\vec r',\alpha,M)e^{i\vec q_\perp\cdot(\vec r-\vec r')}.\end{aligned}\tag{5.1}$$

The principal difference of the inclusive gauge boson production from the diffractive one is in the typical size of the dipoles involved in the scattering. As is seen from, e.g., Eqs. (2.13) and (3.8), the diffractive scattering is dominated by large dipoles scattering at the hadronic scale, with the transverse size $r_p=R_{ij}\sim R_0$ (soft scattering), whereas the inclusive production cross section (5.1) is totally driven by small-size dipoles scattering with $r_p=\alpha r\ll R_0$ (hard scattering). Therefore, different parameterizations for the dipole cross sections must be used—in the diffractive case above we have adopted the Kopeliovich-Schäfer-Tarasov parametrization for the dipole cross section [or the partial amplitude (3.12)] with s-dependent parameters introduced in Eq. (3.13) [13,27], whereas in the inclusive production case the Bjorken x-dependent Golec-Biernat-Wusthofparametrization Eq. (2.13) [21] is better justified:

$$\begin{aligned}&\bar\sigma_0=23.03\ \text{mb},\\&R_0\equiv\bar R_0(x_2)=0.4\ \text{fm}\times(x_2/x_0)^{0.144},\\&x_0=3.04\times10^{-4},\end{aligned}\tag{5.2}$$

where $x_2=q^-/P_2^-$, with P_2 being the 4-momentum of the target proton.

In the leading regime of $\alpha r,\ \alpha r'\ll R_0$,

$$\frac{1}{2}\{\sigma(\alpha r)+\sigma(\alpha r')-\sigma(\alpha|\vec r-\vec r'|)\}\simeq\frac{\alpha^2\bar\sigma_0}{\bar R_0^2(x_2)}(\vec r\cdot\vec r'),\tag{5.3}$$

so the inclusive gauge boson production cross section at forward rapidities ($x_1\gg x_2$) reads

$$\begin{aligned}&\frac{d^4\sigma_{\lambda_G}(pp\to G^*X)}{d^2q_\perp dx_1}\\&=\frac{1}{(2\pi)^2}\frac{\bar\sigma_0}{\bar R_0^2(x_2)}\sum_q\int_{x_1}^1 d\alpha\Big[\rho_q\Big(\frac{x_1}{\alpha}\Big)+\rho_{\bar q}\Big(\frac{x_1}{\alpha}\Big)\Big]\\&\quad\times\int d^2rd^2r'(\vec r\cdot\vec r')\Psi_{V-A}^{\lambda_G}(\vec r,\alpha,M)\\&\quad\times\Psi_{V-A}^{\lambda_G*}(\vec r',\alpha,M)e^{i\vec q_\perp\cdot(\vec r-\vec r')}.\end{aligned}\tag{5.4}$$

We observe that the integrals over α and $\vec r$, $\vec r'$ have the same form as in the diffractive cross section Eq. (4.5).

The M dependence of the differential cross sections for dilepton inclusive production via an intermediate photon γ^* or a gauge boson G^* can be presented similar to the diffractive case, as [32]

$$\frac{d\sigma_{\lambda_\gamma}(pp \to (\gamma^* \to l\bar{l})X)}{d^2q_\perp dx_1 dM^2} = \frac{\alpha_{\rm em}}{3\pi M^2}\frac{d\sigma(pp \to \gamma^* X)}{d^2q_\perp dx_1};$$
$$\frac{d\sigma(pp \to (G^* \to l\bar{l}, l\bar{\nu}_l)X)}{d^2q_\perp dx_1 dM^2} = {\rm Br}(G \to l\bar{l}, l\nu_l) \times \rho_G(M)\frac{d\sigma(pp \to G^* X)}{d^2q_\perp dx_1}, \tag{5.5}$$

where the resonance mass distribution $\rho_G(M)$ is given by Eq. (3.3).

Eventually, we arrive at a simple form for the ratio of the diffractive and inclusive cross sections for dilepton production:

$$\frac{d\sigma^{\rm sd}_{\lambda_G}/d^2q_\perp dx_1 dM^2}{d\sigma^{\rm incl}_{\lambda_G}/d^2q_\perp dx_1 dM^2} = \frac{a^2}{6\pi}\frac{\bar{R}_0^2(M_\perp^2/x_1 s)}{B_{\rm sd}(s)\bar{\sigma}_0}\frac{\sigma_0^2(s)}{R_0^4(s)}\frac{1}{A_2} \times\left[\frac{2}{(A_2-4A_1)^2}+\frac{A_2^2}{(A_2^2-4A_3^2)^2}\right], \tag{5.6}$$

where functions $A_{1,2,3}$ were defined in Eq. (4.6) and fraction x_2 is explicitly given in terms of other kinematic variables in Eq. (4.6).

It turns out that the ratio (5.6) does not depend either on the type of the intermediate boson or on its helicity λ_G. To a good approximation, it is controlled mainly by soft interaction dynamics, in terms of the soft parameters only $\bar{R}_0$, R_0, $\bar{\sigma}_0$, and σ_0. A slow dependence of these parameters on the collision energy s, the hard scale M^2, and the boson transverse momentum $q_\perp$ completely determines such dependence of the diffractive-to-inclusive production ratio. A measurement of the M^2 (or $q_\perp$) dependence of this ratio would allow one to probe the x evolution of the saturation scale, as well as to constrain its energy dependence. Hence, such a quantity is a very useful probe for the underlined QCD diffractive mechanism and the saturation phenomenon and will be quantified based on existing Kopeliovich-Schäfer-Tarasov and Golec-Biernat–Wusthoff parameterizations in the next section.

VI. BREAKDOWN OF DIFFRACTIVE FACTORIZATION

It is instructive to trace the origin of QCD factorization in inclusive processes within the dipole description. The $1/Q^2$ dependence of the DIS cross section at small x originates from two different sources. Most of the $\bar{q}q$ fluctuations of a virtual photon have a small size, $r^2 \sim 1/Q^2$, except the end-point (aligned jet) configurations with $\alpha \to 0$, 1. The latter have large hadronic size and cross section, but their weight is small $\sim 1/Q^2$. Thus, both contributions to the cross section behave as $1/Q^2$.

Similarly, in the Drell-Yan process of radiation of the heavy photon with fractional momentum x_1, the mean size of the artificial dipole [18] has a small size $r \sim 1/(1-\alpha)Q$, except the end-point configurations with $\alpha \to 1$. Like in DIS, α is not an observable but is integrated from x_1 to 1 [see Eq. (5.1)]. This similarity, which reflects the factorization relation between the two processes, also demonstrates its limitations. At large $x_1 \to 1$ the inclusive Drell-Yan reaction is fully dominated by the soft component, and factorization breaks down.

For the diffractive channels, the factorization relation breaks down at any x_1. DIS diffraction is fully dominated by the soft dynamics, since the probability of end-point configurations is still the same, $\propto 1/Q^2$, while the cross section is enhanced by a factor of Q^4 compared with the hard component [5]. However, the mechanism of Drell-Yan diffraction is quite different [15,16], apparently breaking the factorization relation. It comes from the hard-soft interference, which imitates a leading twist throughout the whole range of x_1. Again, like in the inclusive process, the hard and soft (end-point) components make comparable contributions to the diffractive Drell-Yan cross sections. Of course, this is true for other gauge bosons as well.

Although involvement of large distances in diffractive heavy boson production is in obvious contradiction with factorization of hard and soft scales, an observable manifestation of that is not trivial. Indeed, the cross section of a hard process $q\bar{q} \to l\bar{l}$ with the sea quark density in the Pomeron measured in diffractive DIS, although it is a higher twist, imitates the leading twist scale dependence. Nevertheless, the predicted scale and energy dependencies are quite different, as we demonstrate in Sec. VII. Notice that a much more pronounced breakdown of diffractive factorization was previously found in Ref. [14] for the case when the hard scale is imposed by the mass of a heavy flavor.

VII. NUMERICAL RESULTS

We now turn to a discussion of the numerical results for the most important observables. First of all, we are interested in the dilepton (*à la* Drell-Yan pair) production channel as the simplest one. Although the quark production channel could also be of interest, this case will be considered elsewhere.

In Figs. 1 (for RHIC energy $\sqrt{s} = 500$ GeV) and 2 (for LHC energy $\sqrt{s} = 14$ TeV), we present the single diffractive cross sections for Z^0, γ^* (diffractive DY), and $W^\pm$ boson production, differential in the dilepton mass squared $d\sigma_{\rm sd}/dM^2$ (left panels) and its longitudinal momentum fraction $d\sigma_{\rm sd}/dx_1$ (right panels). These plots do not reflect particular detector constraints—a thorough analysis including detector acceptances and cuts has to be done separately. The M^2 distributions here are integrated over the *ad hoc* interval of fractional boson momentum $0.3 < x_1 < 1$, corresponding to the forward rapidity region (at not

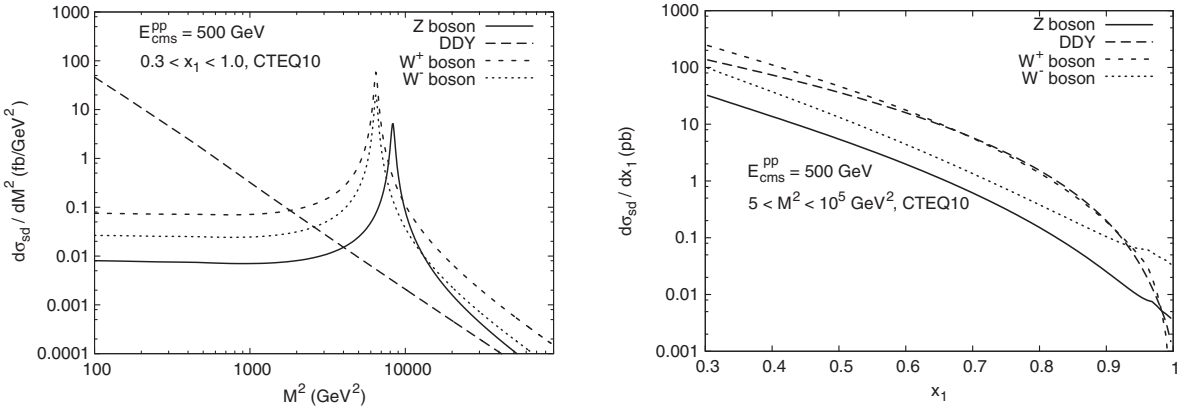

FIG. 1. Diffractive gauge boson production cross section as a function of the dilepton invariant mass squared M^2 (left panel) and boson fractional light-cone momentum x_1 (right panel) in pp collisions at the RHIC energy $\sqrt{s} = 500$ GeV. Solid, long-dashed, dashed, and dotted curves correspond to Z, γ^*, W^+, and W^- bosons, respectively. CTEQ10 parton distribution function (PDF) parametrization [33] is used here.

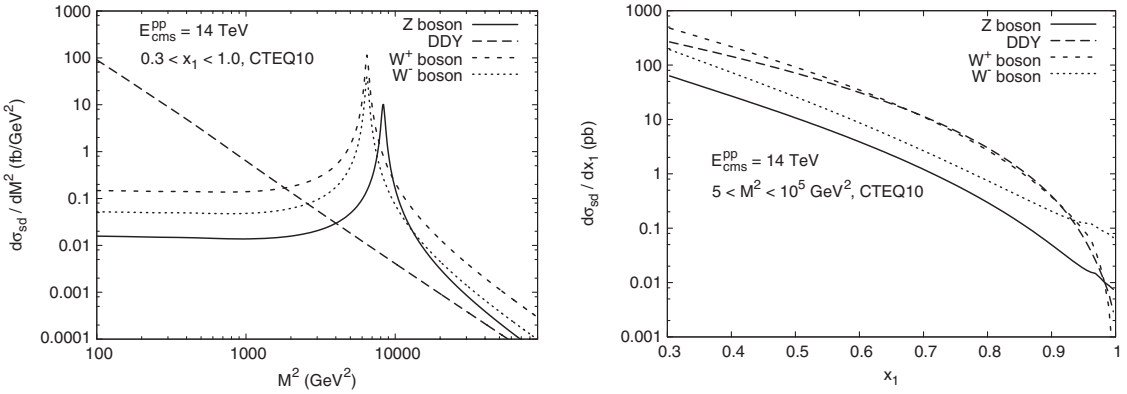

FIG. 2. The same as in Fig. 1, but for the LHC energy $\sqrt{s} = 14$ TeV.

extremely large masses). Then the mass distribution is integrated over the potentially interesting invariant mass interval $5 < M^2 < 10^5$ GeV^2 and can be easily converted into (pseudo)rapidity ones widely used in experimental studies, if necessary.

The M^2 distributions of the Z^0 and $W^\pm$ bosons clearly demonstrate their resonant behavior and, in the resonant region, significantly exceed the corresponding diffractive Drell-Yan component; only for very low masses does the γ^* contribution become important (left panels). For x_1 distribution, when integrated over low mass and resonant regions, diffractive W^+ and γ^* components become comparable to each other, in both shapes and values, whereas the W^- and, especially, Z boson production cross section are noticeably lower (right panels). Quite naturally, the W^- cross section is (in analogy with the well-known inclusive $W^\pm$ production) smaller than the W^+ one due to differences in valence u- and d-quark densities (dominating over sea quarks at large x_q) in the proton to which the bosons couple. So the precise measurement of differences in forward diffractive W^+ and W^- rates would allow one to constrain quark content of the proton at large $x_q \equiv x_1/\alpha$. In Figs. 1 and 2, and in all calculations below, we have used the most recent CTEQ10 valence or sea quark PDF parametrization [33], if not declared otherwise.

In Fig. 3, we show the ratio of the longitudinal (L) to transverse (T) gauge boson polarization contributions to the diffractive production cross section. This ratio is presented differentially as a function of lepton-pair invariant mass squared $(\sigma^L_{sd}/dM^2)/(\sigma^T_{sd}/dM^2)$ (left panel) and gauge boson fractional momentum $(\sigma^L_{sd}/dx_1)/(\sigma^T_{sd}/dx_1)$ (right panel). We see that the diffractive gauge boson production process is always dominated by radiation of transversely polarized lepton pairs. The ratio σ_L/σ_T only slightly depends on M^2 and even less on pp c.m. energy $\sqrt{s}$, so it can be considered as energy independent [which, in fact, can be already seen from approximate formulas (4.9) and (4.10)]. The longitudinal boson polarization roughly amounts to 10% at $x_1 \sim 0.5$ and then steeply falls down at large $x_1 \to 1$ asymptotically approaching the

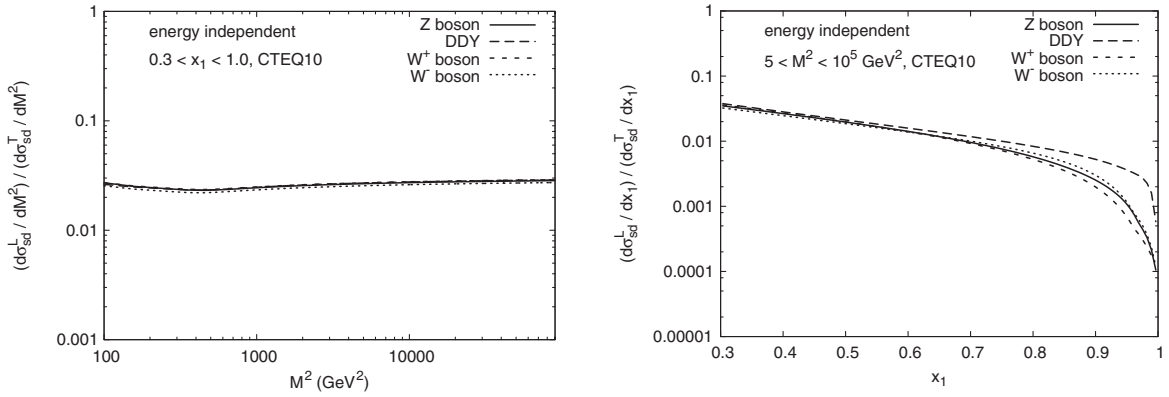

FIG. 3. The ratio of the cross sections of longitudinally (L) to transversely (T) polarized gauge bosons, as a function of the dilepton invariant mass squared M^2 (left panel) and boson fractional light-cone momentum x_1 (right panel). Solid, long-dashed, dashed, and dotted curves correspond to Z, γ^*, W^+, and W^- bosons, respectively. CTEQ10 PDF parametrization [33] is used here. The ratio depends on pp c.m. energy only slightly, by a few percent (cf. Ref. [16]) over a vast multi-TeV interval, so we neglect it here.

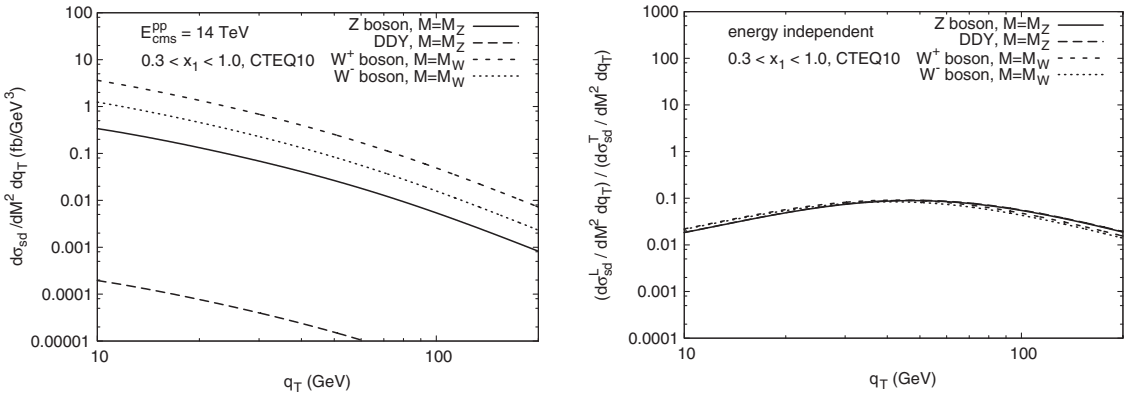

FIG. 4. The dilepton transverse momentum $q_\perp$ distribution of the doubly differential diffractive cross section at the LHC energy $\sqrt{s} = 14$ TeV at a fixed dilepton invariant mass is shown in the left panel. The longitudinal-to-transverse gauge boson polarization ratio as a function of the dilepton $q_\perp$ is shown in the right panel. In both panels, the invariant mass is fixed as $M = M_Z$ in the Z^0, γ^* production case and as $M = M_W$ in the $W^\pm$ production case. CTEQ10 PDF parametrization [33] is used here.

relativistic (massless) boson case given, due to the gauge invariance, by the transverse polarization only. Such a behavior turns out to be the same as in the inclusive Drell-Yan process [15]. At smaller $x_1 \lesssim 0.6$, this ratio becomes the same for different bosons, whereas at large $x_1 \to 1$ the relative contribution of the longitudinally polarized photon dominates in corresponding ratios for other bosons.

From the phenomenological point of view, the distribution of the forward diffractive cross section in the dilepton transverse momentum $q_\perp$ could also be of major importance.[4] In Fig. 4 (left panel), we show the dilepton transverse momentum $q_\perp$ distribution of the doubly differential diffractive cross section at the LHC energy $\sqrt{s} = 14$ TeV at the dilepton invariant mass, fixed at a corresponding resonance value—the Z or W mass. The shapes turned out to be smooth and the same for different gauge bosons and are different mostly in normalization. In Fig. 4 (right panel), we show the $q_\perp$ dependence of the σ^L/σ^T ratio in the resonances. We notice that the ratio does not strongly vary for different bosons. It is peaked at about half of the resonance mass and uniformly decreases to smaller or larger $q_\perp$ values.

As one of the important observables, sensitive to the difference between u- and d-quark PDFs, the $W^\pm$ charge asymmetry A_W is shown in Fig. 5 differentially as a function of the dilepton invariant mass squared M^2 and integrated over the $0.3 < x_1 < 1.0$ interval (left panel):

$$A_W(M^2) = \frac{d\sigma_{\rm sd}^{W^+}/dM^2 - d\sigma_{\rm sd}^{W^-}/dM^2}{d\sigma_{\rm sd}^{W^+}/dM^2 + d\sigma_{\rm sd}^{W^-}/dM^2}, \tag{7.1}$$

and as a function of the boson momentum fraction x_1 and integrated over the $5 < M^2 < 10^5$ GeV^2 interval (right panel):

[4]The authors are indebted to Torbjörn Sjöstrand for pointing this out.

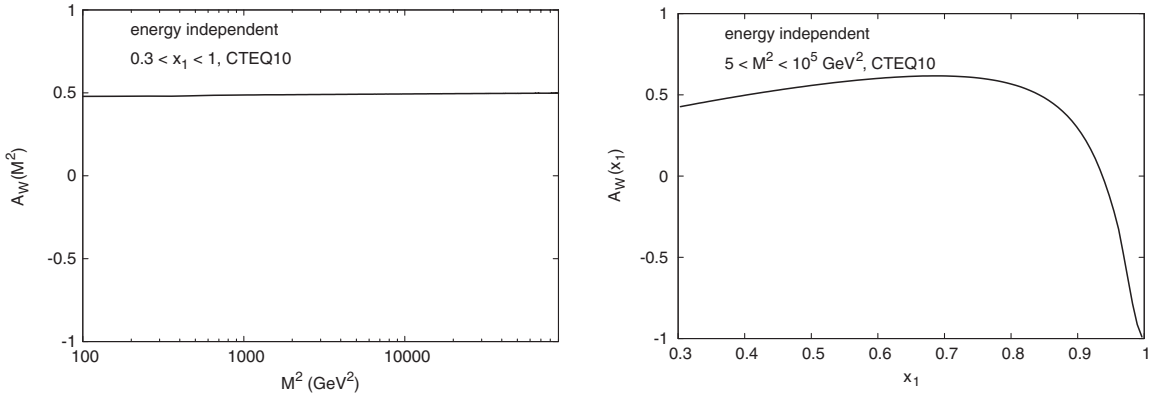

FIG. 5. Charge asymmetry in the single diffractive W^+ and W^- cross sections as a function of M^2, at fixed $x_1 = 0.5$ (left panel), and x_1, at fixed $M^2 = M_W^2$ (right panel). Solid lines correspond to the LHC energy $\sqrt{s} = 14$ TeV and dashed lines to the RHIC energy $\sqrt{s} = 500$ GeV.

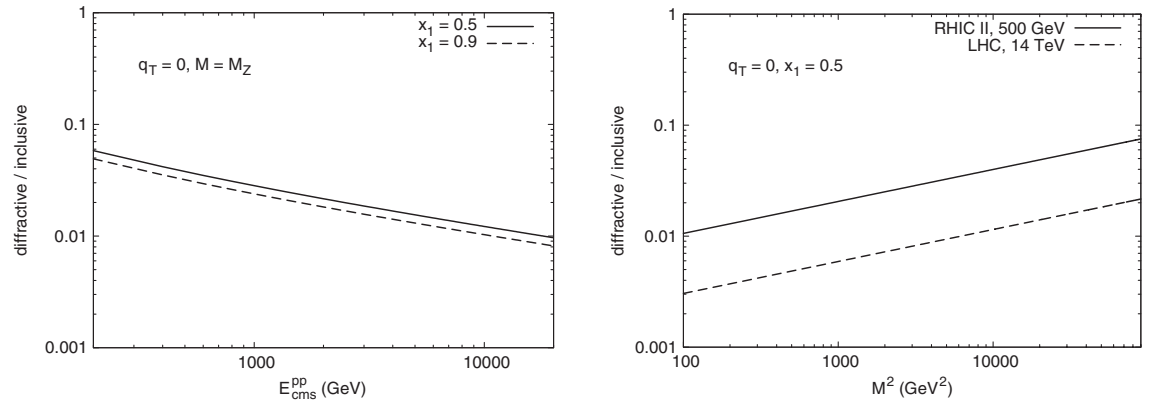

FIG. 6. The diffractive-to-inclusive ratio of the gauge boson production cross sections in pp collisions derived in Eq. (5.6) as a function of the c.m. energy $\sqrt{s}$ (left panel) and the dilepton invariant mass M^2 (right panel). It does not depend on the type of the gauge boson and quark PDFs.

$$A_W(x_1) = \frac{d\sigma_{\rm sd}^{W^+}/dx_1 - d\sigma_{\rm sd}^{W^-}/dx_1}{d\sigma_{\rm sd}^{W^+}/dx_1 + d\sigma_{\rm sd}^{W^-}/dx_1}. \tag{7.2}$$

The ratio turns out to be independent on both the hard scale M^2 and the c.m. energy $\sqrt{s}$. One concludes that, due to different x shapes of valence u- and d-quark PDFs, at smaller $x_1 \lesssim 0.9$ the diffractive W^+ bosons' rate dominates over the W^- one. However, at large $x_1 \to 1$ the W^- boson cross section becomes increasingly important and strongly dominates over the W^+ one.

An important feature of the diffractive-to-inclusive Abelian radiation cross section ratio

$$R(M^2, x_1) = \frac{d\sigma_{\rm sd}/dx_1 dM^2}{d\sigma_{\rm incl}/dx_1 dM^2}, \tag{7.3}$$

which makes these predictions different from ones obtained in traditional diffractive QCD factorization-based approaches (see, e.g., Refs. [11,12]), is their unusual energy and scale dependence demonstrated in Fig. 6. Notice that we stick to the case of small boson transverse momenta, $q_\perp \ll M$, where the main bulk of diffractive signals come from. The analytic formula for this ratio was derived above and is shown by Eq. (5.6), which demonstrates that the ratio is independent of the type of the gauge boson, its polarization, or quark PDFs. In this respect, it is the most convenient and model independent observable, which is sensitive only to the structure of the universal elastic dipole amplitude (or the dipole cross section), and can be used as an important probe for the QCD diffractive mechanism for forward diffractive reactions, essentially driven by the soft interaction dynamics. We see from Fig. 6 that the $\sigma_{\rm sd}/\sigma_{\rm incl}$ ratio decreases with energy but increases with the hard scale and, thus, behaves opposite to what is expected in the diffractive factorization-based approaches. Therefore, measurements of the single diffractive gauge boson production cross section, at least, at two different energies would provide important information about the interplay between soft and hard interactions in QCD and its role in the formation of diffractive excitations and color screening effects.

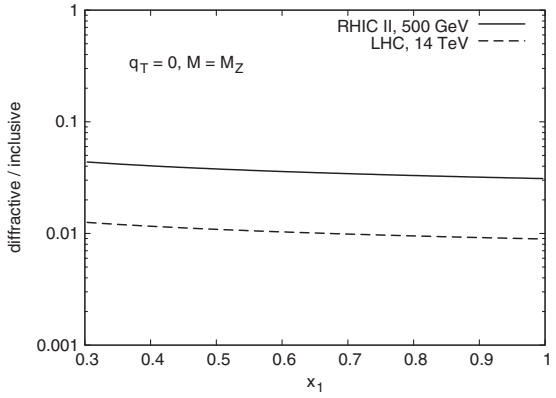

FIG. 7. The diffractive-to-inclusive ratio as a function of the boson fractional momentum x_1.

Finally, in Fig. 7, we present the diffractive-to-inclusive cross section ratio as a function of the boson fractional momentum x_1 at RHIC ($\sqrt{s} = 500$ GeV) and at LHC ($\sqrt{s} = 14$ TeV) energies (left panel). In the right panel, we compare this ratio calculated at the Tevatron energy ($\sqrt{s} = 1.96$ TeV) with the recent measurements of diffractive W and Z production performed by the CDF Collaboration [9]. The data show the x_1-integrated ratio of diffractive-to-inclusive cross sections. Because of the weak x_1 dependence of this ratio (left panel), with a good accuracy the integrated values are numerically close to the ratio of differential cross sections given by Eq. (7.3). We see that the results of our calculations with Eq. (5.6) at $x_1 = 0, 5$ agree well with the data. This agreement is another confirmation of correctness of the absorption effects included into the parametrization of the dipole cross section (3.12).

VIII. THE RESULTS MEET DATA

A. Link to the Regge phenomenology and data

The process $pp \to Xp$ at large Feynman $x_F \to 1$ of the recoil proton, or small

$$\xi = 1 - x_F = \frac{M_X^2}{s} \ll 1, \tag{8.1}$$

is described by triple-Regge graphs $\mathbb{PPP}$ and $\mathbb{PPR}$ depicted in Figs. 8, (aa) and (ab) respectively, where we also included radiation of a gauge boson. Examples of Feynman graphs corresponding to the above triple-Regge terms are shown in the second and third rows in Fig. 8. The graphs (ba) and (ca) illustrate the triple-Pomeron term in the diffraction cross section

$$\frac{d\sigma_{\rm diff}^{\mathbb{PPP}}}{d\xi dt} \propto \xi^{-\alpha_{\mathbb{P}}(0)-2\alpha'_{\mathbb{P}}(t)}, \tag{8.2}$$

with the gauge boson radiated by either a sea (ba) or a valence (ca) quark. The effective radiation amplitude $q + g \to q + G$ is depicted by open circles and is defined in

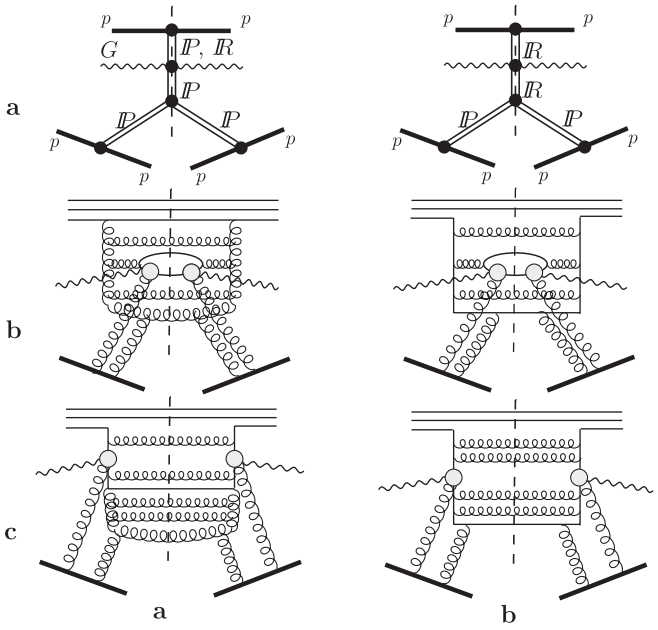

FIG. 8. Upper row: The triple-Regge graphs for the process $pp \to Xp$, where the diffractively produced state X contains a gauge boson. Examples of Feynman graphs corresponding to diffractive excitation of a large invariant mass, going along with radiation of a gauge boson, are displayed in the 2nd and 3rd rows. Curly and waving lines show gluons and the radiated gauge boson, respectively. The dashed line indicates the unitarity cut.

Fig. 9. These Feynman graphs interpret the triple-Pomeron term as a diffractive excitation of the incoming proton due to radiation of gluons with small fractional momentum. The proton can also dissociate via diffractive excitation of its valence quark skeleton, as is illustrated in Figs. 8 (bb) and (cb). The corresponding term in the diffraction cross section reads

$$\frac{d\sigma_{\rm diff}^{\mathbb{PPR}}}{d\xi dt} \propto \xi^{\alpha_{\mathbb{R}}(0)-\alpha_{\mathbb{P}}(0)-2\alpha'_{\mathbb{P}}(t)}. \tag{8.3}$$

Again, the gauge boson can be radiated either by a sea quark (bb) or by the valence (cb) quark.

It is worth emphasizing that the quark radiating the gauge boson cannot be a spectator but must participate in the interaction. This is a straightforward consequence of the Good-Walker mechanism of diffraction [3]. As was discussed above, the contribution of a given projectile Fock state to the diffraction amplitude is given by the difference

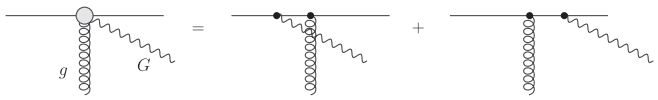

FIG. 9. The effective amplitude of gauge boson radiation by a projectile quark.

of elastic amplitudes for the Fock states including or excluding the gauge boson:

$$\mathrm{Im}\, f_{\mathrm{diff}}^{(n)} = \mathrm{Im} f_{\mathrm{el}}^{(n+G)} - \mathrm{Im} f_{\mathrm{el}}^{(n)}, \tag{8.4}$$

where n is the total number of partons in the Fock state; $f_{\mathrm{el}}^{(n+G)}$ and $f_{\mathrm{el}}^{(n)}$ are the elastic scattering amplitudes for the whole n-parton ensemble, which either contains the gauge boson or does not, respectively. Although the gauge boson does not participate in the interaction, the impact parameter of the quark radiating the boson gets shifted, and this is the only reason why the difference Eq. (8.4) is not zero. This also conveys that this quark must interact in order to retain the diffractive amplitude nonzero [15]. For this reason, in the graphs depicted in Fig. 8, the quark radiating G always takes part in the interaction with the target.

Notice that there is no one-to-one correspondence between diffraction in QCD and the triple-Regge phenomenology. In particular, there is no triple-Pomeron vertex localized in rapidity. The colorless "Pomeron" contains at least two t-channel gluons, which can couple to any pair of projectile partons. For instance, in diffractive gluon radiation, which is the lowest order term in the triple-Pomeron graph, one of the t-channel gluons can couple to the radiated gluon, while another one couples to another parton at any rapidity, e.g., to a valence quark (see Fig. 3 in Ref. [13]). Apparently, such a contribution cannot be associated literally with either of the Regge graphs in Fig. 8. Nevertheless, this does not affect much the x_F and energy dependencies provided by the triple-Regge graphs, because the gluon has spin one.

It is also worth mentioning that in Fig. 8 we presented only the lowest order graphs with two-gluon exchange. The spectator partons in a multiparton Fock component also can interact and contribute to the elastic amplitude of the whole parton ensemble. This gives rise to higher order terms, not shown explicitly in Fig. 8. They contribute to the diffractive amplitude Eq. (8.4) as a factor, which we define as the gap survival amplitude.

B. Gap survival amplitude

The amplitude of survival of a large rapidity gap is controlled by the largest dipoles in the projectile hadron. This was included in our evaluation of the diffractive amplitude Eq. (4.11). Soft gluons in the light-cone wave function of the proton should also be considered as spectator partons, and the large (compared with $1/M_G$) distance R_{ij} in Eq. (4.1) in this case is the quark-gluon separation. In fact, our calculations do include such configurations. Indeed, data on diffraction show that diffractive gluon radiation is quite weak (well known smallness of the triple-Pomeron coupling), and this can be explained by assuming that gluons in the proton are located within small "spots" around the valence quarks with radius $r_0 \sim 0.3$ fm [13,34–36]. Therefore, the large distance between one valence quark and a satellite gluon of the other quark is approximately equal (with 10% accuracy) to the quark-quark separation. Since a valence quark together with comoving gluons is a color triplet, in our calculations the interaction amplitude of such an effective ("constituent") quark with the target is a coherent sum of the quark-target and gluon-target interaction amplitudes.

In addition to the soft gluons, which are present in the proton light-cone wave function at a soft scale, production of a heavy gauge boson certainly leads to an additional intensive hard gluon radiation. In other words, there might be many more spectator gluons in the quark which radiates the gauge boson. The transverse separation of those gluons is controlled by the Dokshitzer-Gribov-Lipatov-Altarelli-Parisi evolution. One can replace a bunch of gluons by dipoles [37] whose transverse size r_d varies from $1/M_G$ up to r_0 and is distributed as dr_d/r_d [38]. Therefore the mean dipole size squared

$$\langle r_d^2 \rangle = \frac{r_0^2}{\ln(r_0^2 M_G^2)} \tag{8.5}$$

is about $\langle r_d^2 \rangle \approx 0.01$ fm^2, i.e., quite small. The cross section of such a dipole on a proton is also small, $\sigma_d = C(x)\langle r_d \rangle^2$, where according to Eq. (2.13) a factor $C(x) = \sigma_0/R_0^2(x)$ rises with energy. Fixing $x = M_G^2/s$ and using the parameters fitted in Ref. [21] to DIS data from HERA, we get at the Tevatron collider energy $\sigma_d \approx 0.9$ mb.

The presence of each such dipole in the projectile light-cone wave function brings an extra suppression factor to the survival amplitude of a large rapidity gap:

$$S_d(s) = 1 - \mathrm{Im} f_d(b, r_d). \tag{8.6}$$

We aimed here at a demonstration that the second term in (8.6) is negligibly small, so we rely on its simplified form (see the more involved calculations in Ref. [39])

$$\mathrm{Im}\, f_d(b, r_d) \approx \frac{\sigma_d}{4\pi B_d} e^{-b^2/2B_d}, \tag{8.7}$$

where B_d is the dipole-nucleon elastic slope, which was measured at $B_d \approx 6$ GeV^{-2} in diffractive electroproduction of ρ mesons at HERA [40].

We evaluate the absorptive correction (8.7) at the mean impact parameter $\langle b^2 \rangle = 2B_d$ and for the Tevatron energy $\sqrt{s} = 2$ TeV arrive at the negligibly small value $\mathrm{Im} f_d(0, r_d) \approx 0.01$.

However, the number of such dipoles rises with hardness of the process and may substantially enhance the magnitude of the absorptive corrections. The gap survival amplitude for n_d projectile dipoles reads

$$S_d^{(n_d)} = [1 - \mathrm{Im} f_d(b, r_d)]^{n_d}. \tag{8.8}$$

The mean number of dipoles can be estimated in the double-leading-log approximation to the Dokshitzer-Gribov-Lipatov-Altarelli-Parisi evolution formulated in impact parameters [38]; the mean number of such dipoles is given by

$$\langle n_d \rangle = \sqrt{\frac{12}{\beta_0} \ln\left(\frac{1}{\alpha_s(M_G^2)}\right) \ln\left((1-x_F)\frac{s}{s_0}\right)}. \tag{8.9}$$

Here the values of Bjorken x of the radiated gluons is restricted by the invariant mass of the diffractive excitation, $x > s_0/M_X^2 = s_0/(1-x_F)s$. For the kinematics of experiments at the Tevatron collider (see the next section), $1 - x_F < 0.1$, $\sqrt{s} = 2$ TeV, the number of radiated dipoles is not large: $\langle n_d \rangle \lesssim 6$. We conclude that the absorptive corrections Eq. (8.8) to the gap survival amplitude are rather weak, less than 5%, i.e., about 10% in the survival probability. This correction is certainly small compared to other theoretical uncertainties of our calculations. Notice that a similar correction due to radiation of soft gluons was found in Ref. [39] for the gap survival probability in leading neutron production in DIS.

C. Comparison with data

Thus, our calculations effectively cover the gluon radiation, so the triple-Pomeron term is included. This is important, because this term dominates the diffractive cross section [41]. So we can compare with available data from the CDF experiment [9] on W and Z diffractive production depicted in Fig. 10.

However, in order to compare our results with CDF data, we have to introduce in our calculations the proper experimental cuts, namely, $0.03 < \xi \equiv 1 - x_F < 0.1$ [9]. Since our diffractive cross section formulas are differential in M^2, not in M_X^2, and experimental cuts on y-rapidity distribution of a produced gauge boson are unavailable at the moment, a direct implementation of the ξ cuts into our formalism cannot be performed immediately.

As a way out of this problem, at small $\xi \to 0$ one can instead write the single diffractive cross section in the phenomenological triple-Regge form [41]

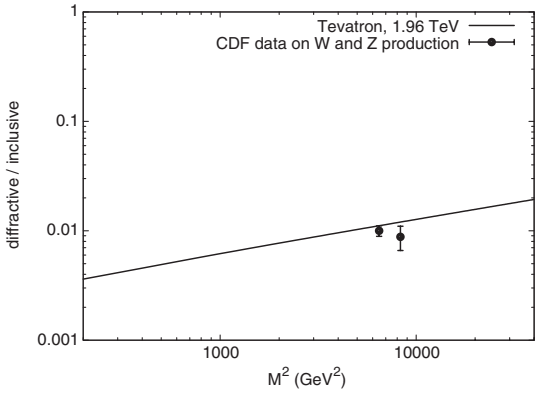

FIG. 10. The diffractive-to-inclusive ratio as a function of the invariant mass squared of the produced dilepton. The CDF data for W and Z production were taken at the Tevatron energy ($\sqrt{s} = 1.96$ TeV). The first CDF data point corresponds to the W production, $M^2 = M_W^2$, and the second to the Z production, $M^2 = M_Z^2$.

$$-\frac{d\sigma_{\rm sd}^{pp}}{d\xi dp_T^2} = \sqrt{\frac{s_1}{s}} \frac{G_{\mathbb{PPR}}(0)}{\xi^{3/2}} e^{-B_{\mathbb{PPR}} p_T^2} + \frac{G_{3\mathbb{P}}(0)}{\xi} e^{-B_{3\mathbb{P}}^{pp} p_T^2}, \tag{8.10}$$

where $s_1 = 1$ GeV^2; $B_{\mathbb{PP}i} = R_{\mathbb{PP}i}^2 - 2\alpha'_{\mathbb{P}} \ln\xi$; $i = \mathbb{P}, \mathbb{R}$; and $\alpha'_{\mathbb{P}} \approx 0.25$ GeV^{-2} is the slope of the Pomeron trajectory. Then an effect of the experimental cuts on ξ in the phenomenological cross section (8.10) and in our diffractive cross section calculated above (3.6) should roughly be the same.

Since the data show no substantial rise of the diffractive cross section with energy [42,43], which is apparently caused by strong absorptive corrections, we incorporate this fact by fixing the effective Pomeron intercept at $\alpha_{\mathbb{P}}(0) = 1$. This also allows us to use the results of the comprehensive triple-Regge analysis of data performed in Ref. [41], which led to the following values of the parameters: $G_{3\mathbb{P}}(0) = G_{\mathbb{PPR}}(0) = 3.2$ mb/GeV^2; $R_{3\mathbb{P}}^2 = 4.2$ GeV^{-2}; $R_{\mathbb{PPR}}^2 = 1.7$ GeV^{-2}.

Now we are in a position to evaluate the suppression factor δ caused by the experimental cut on ξ, by taking the ratio

$$\delta = \frac{\int dp_T^2 \int_{0.03}^{0.1} d\xi d\sigma/dp_T^2 d\xi}{\int dp_T^2 \int_{\xi_{\rm min}}^{\xi_{\rm max}} d\xi d\sigma/dp_T^2 d\xi}. \tag{8.11}$$

Here $\xi_{\rm min} = M_{X,\rm min}^2/s$, where $M_{X,\rm min} \simeq M_Z$ is the minimal produced diffractive mass containing a heavy gauge boson. The value of δ in Ref. (8.11) is essentially determined by the experimental cuts on ξ and is not sensitive to the upper limit $\xi_{\rm max}$ in the denominator, so we fix it at a realistic value:[5] $\xi_{\rm max} \sim 0.3$. Then Eq. (8.11) leads to $\delta \simeq 0.2$, the factor reducing the diffractive gauge boson production cross section calculated above. Our result plotted in Fig. 10 demonstrates a good agreement with the CDF data on single diffractive W and Z production [9].

IX. CONCLUSIONS

The diffractive radiation of Abelian fields, γ, Z^0, and $W^\pm$, expose unusual features, which make it very different from diffraction in DIS, and lead to a dramatic breakdown of QCD factorization in diffraction.

The first, rather obvious source for violation of diffractive factorization is related to absorptive corrections (called sometimes survival probability of large rapidity gaps). The absorptive corrections affect differently the diagonal and off-diagonal terms in the hadronic current

[5]The estimate for $\xi_{\rm max} \sim 0.3$ corresponds to the limiting case when one of the constituent quarks in a target (anti)proton loses almost all its energy into a hard radiation of a gluon in the t channel. The second and all subsequent t-channel gluon exchanges collectively screen the color charge taken away from the target by the first gluon and transfer a much smaller fraction of initial target momentum to projectile quarks as has been recently advocated in Refs. [44,45].

[46], leading to an unavoidable breakdown of QCD factorization in processes with off-diagonal contributions only. Namely, the absorptive corrections suppress the off-diagonal diffraction much more strongly than the diagonal channels. In the diffractive Abelian radiation in hadron-hadron collisions, a new state, i.e., the gauge boson decaying into the heavy lepton pair, is produced, and, hence, the whole process is of entirely off-diagonal nature, whereas in the diffractive DIS contains both diagonal and off-diagonal contributions [4]. This is the first reason why QCD factorization is broken in the diffractive gauge boson production processes.

The second, more sophisticated reason to contradict diffractive factorization is specific for Abelian radiation; namely, a quark cannot radiate in the forward direction (zero momentum transfer), where diffractive cross sections usually have a maximum. Forward diffraction becomes possible due to intrinsic transverse motion of quarks inside the proton.

Third, the mechanism of Abelian radiation in the forward direction in pp collisions is related to participation of the spectator partons in the proton. Namely, the perturbative QCD interaction of a projectile quark is responsible for the hard process of a heavy boson radiation, while a soft interaction with the projectile spectator partons provides color neutralization [44,45], which is required for a diffractive (Pomeron exchange) process. Such an interplay of hard and soft dynamics is also specific for the process under consideration, which makes it different from the diffractive DIS, dominated exclusively by soft interactions, and which also results in breakdown of diffractive factorization.

The diffractive (Ingelman-Schlein) QCD factorization breaking manifests itself in specific features of diffractive observables like a significant damping of the single diffractive gauge boson production cross section at high $\sqrt{s}$ compared to the inclusive production case. This is rather unusual, since a diffractive cross section, which is proportional to the dipole cross section squared, could be expected to rise with energy steeper than the total inclusive cross section, like it occurs in the diffractive DIS process. At the same time, the ratio of the single diffractive-to-inclusive production cross sections rises with the hard scale M^2. This is also in variance with diffraction in DIS associated with the soft interactions.

In this paper, we have presented the differential distributions (in transverse momentum, invariant mass, and longitudinal momentum fraction) of the diffractive γ^*, Z^0, and $W^\pm$ boson production at RHIC (500 GeV) and LHC (14 TeV) energies, as well as the ratio of the boson longitudinal-to-transverse polarization contributions. We have also calculated the charge $W^\pm$ asymmetry, relevant for upcoming measurements at the LHC. The ratio of diffractive-to-inclusive gauge boson production cross sections does not depend on a particular type of gauge boson, its polarization state, and quark PDFs and depends only on properties of the universal dipole cross section and sensitive to the saturation scale at small x. Finally, our prediction for this ratio is numerically consistent with the one measured for diffractive W and Z production at the Tevatron.

The theoretical uncertainties of our calculations come mainly from poorly known quark PDFs [or the proton structure function $F_2(x_q)$ in diffractive DY (DDY)] at large quark fractions $x_q \to 1$. This issue has been discussed in our previous analysis of the DDY process in Ref. [16], where a strong sensitivity of the x_1 dependence to a particular F_2 parametrization has been pointed out. The same situation extends to the more general case of diffractive Abelian radiation considered in this paper. This tells us again that measurements of forward diffractive gauge boson production would be extremely important or even crucial for settling further more stringent constraints on the quark content of the proton.

ACKNOWLEDGMENTS

Useful discussions and helpful correspondence with Gunnar Ingelman, Valery Khoze, Yuri Kovchegov, Eugene Levin, Amir Rezaeian, Christophe Royon, Torbjörn Sjöstrand, and Antoni Szczurek are gratefully acknowledged. This study was partially supported by Fondecyt (Chile) Grant No. 1090291 and by Conicyt-DFG Grant No. 084-2009.

[1] R. J. Glauber, Phys. Rev. **100**, 242 (1955).
[2] E. Feinberg and I. Ya. Pomeranchuk, Nuovo Cimento Suppl. **3**, 652 (1956).
[3] M. L. Good and W. D. Walker, Phys. Rev. **120**, 1857 (1960).
[4] B. Z. Kopeliovich, I. K. Potashnikova, and I. Schmidt, Braz. J. Phys. **37**, 473 (2007).
[5] B. Z. Kopeliovich and B. Povh, Z. Phys. A **356**, 467 (1997).
[6] B. Z. Kopeliovich, L. I. Lapidus, and A. B. Zamolodchikov, Pis'ma Zh. Eksp. Teor. Fiz. **33**, 612 (1981); [JETP Lett. **33**, 595 (1981)].
[7] G. Ingelman and P. E. Schlein, Phys. Lett. B **152**, 256 (1985).
[8] F. Abe *et al.* (CDF Collaboration), Phys. Rev. Lett. **78**, 2698 (1997).
[9] T. Aaltonen *et al.* (CDF Collaboration), Phys. Rev. D **82**, 112004 (2010).

[10] K. A. Goulianos, arXiv:hep-ph/9708217.
[11] G. Kubasiak and A. Szczurek, Phys. Rev. D **84**, 014005 (2011).
[12] M. B. Gay Ducati, M. M. Machado, and M. V. T. Machado, Phys. Rev. D **75**, 114013 (2007).
[13] B. Z. Kopeliovich, A. Schäfer, and A. V. Tarasov, Phys. Rev. D **62**, 054022 (2000).
[14] B. Z. Kopeliovich, I. K. Potashnikova, I. Schmidt, and A. V. Tarasov, Phys. Rev. D **76**, 034019 (2007).
[15] B. Z. Kopeliovich, I. K. Potashnikova, I. Schmidt, and A. V. Tarasov, Phys. Rev. D **74**, 114024 (2006).
[16] R. S. Pasechnik and B. Z. Kopeliovich, arXiv:1109.6690; Eur. Phys. J. C **71**, 1827 (2011).
[17] S. J. Brodsky, A. Hebecker, and E. Quack, Phys. Rev. D **55**, 2584 (1997).
[18] B. Z. Kopeliovich, in *Proceedings of the International Workshop XXIII on Gross Properties of Nuclei and Nuclear Excitations, Hirschegg, Austria, 1995*, edited by H. Feldmeyer and W. Nörenberg (Gesellschaft für Schwerionenforschung, Darmstadt, 1995), p. 385.
[19] B. Z. Kopeliovich, A. V. Tarasov, and A. Schafer, Phys. Rev. C **59**, 1609 (1999).
[20] S. J. Brodsky and P. Hoyer, Phys. Lett. B **298**, 165 (1993).
[21] K. J. Golec-Biernat and M. Wusthoff, Phys. Rev. D **59**, 014017 (1998).
[22] J. Bartels, K. J. Golec-Biernat, and H. Kowalski, Phys. Rev. D **66**, 014001 (2002).
[23] V. I. Kuksa and R. S. Pasechnik, Int. J. Mod. Phys. A **23**, 4125 (2008); Phys. At. Nucl. **73**, 1622 (2010); Mod. Phys. Lett. A **26**, 1075 (2011).
[24] K. Nakamura *et al.* (Particle Data Group Collaboration), J. Phys. G **37**, 075021 (2010).
[25] B. Z. Kopeliovich, H. J. Pirner, A. H. Rezaeian, and I. Schmidt, Phys. Rev. D **77**, 034011 (2008).
[26] B. Z. Kopeliovich, I. K. Potashnikova, I. Schmidt, and J. Soffer, Phys. Rev. D **78**, 014031 (2008).
[27] B. Z. Kopeliovich, A. H. Rezaeian, and I. Schmidt, Phys. Rev. D **78**, 114009 (2008).
[28] R. M. Barnett *et al.*, Rev. Mod. Phys. **68**, 611 (1996).
[29] S. Amendolia *et al.*, Nucl. Phys. **B277**, 168 (1986).
[30] G. T. Garvey and J.-C. Peng, Prog. Part. Nucl. Phys. **47**, 203 (2001).
[31] A. H. Mueller, Nucl. Phys. **A715**, 20c (2003); A. H. Mueller and D. N. Triantafyllopoulos, Nucl. Phys. **B640**, 331 (2002).
[32] B. Z. Kopeliovich, J. Raufeisen, and A. V. Tarasov, Phys. Lett. B **503**, 91 (2001).
[33] H. L. Lai, M. Guzzi, J. Huston, Z. Li, P. M. Nadolsky, J. Pumplin, and C. P. Yuan, Phys. Rev. D **82**, 074024 (2010).
[34] T. Schafer and E. V. Shuryak, Rev. Mod. Phys. **70**, 323 (1998).
[35] E. Shuryak and I. Zahed, Phys. Rev. D **69**, 014011 (2004).
[36] B. Z. Kopeliovich, I. K. Potashnikova, B. Povh, and I. Schmidt, Phys. Rev. D **76**, 094020 (2007).
[37] A. H. Mueller and B. Patel, Nucl. Phys. **B425**, 471 (1994).
[38] N. N. Nikolaev and B. G. Zakharov, Zh. Eksp. Teor. Fiz. **105**, 1117 (1994); [J. Exp. Theor. Phys. **78**, 598 (1994)].
[39] B. Z. Kopeliovich, I. K. Potashnikova, B. Povh, and I. Schmidt, Phys. Rev. D **85**, 114025 (2012).
[40] S. Chekanov *et al.* (ZEUS Collaboration), PMC Phys. A **1**, 6 (2007).
[41] Yu. M. Kazarinov, B. Z. Kopeliovich, L. I. Lapidus, and I. K. Potashnikova, J. Exp. Theor. Phys. **70**, 1152 (1976).
[42] K. Goulianos and J. Montanha, Phys. Rev. D **59**, 114017 (1999).
[43] S. Erhan and P. E. Schlein, Phys. Lett. B **427**, 389 (1998).
[44] R. Pasechnik, R. Enberg, and G. Ingelman, Phys. Rev. D **82**, 054036 (2010).
[45] R. Pasechnik, R. Enberg, and G. Ingelman, Phys. Lett. B **695**, 189 (2011).
[46] B. Z. Kopeliovich, I. K. Potashnikova, I. Schmidt, and M. Siddikov, Phys. Rev. C **84**, 024608 (2011).